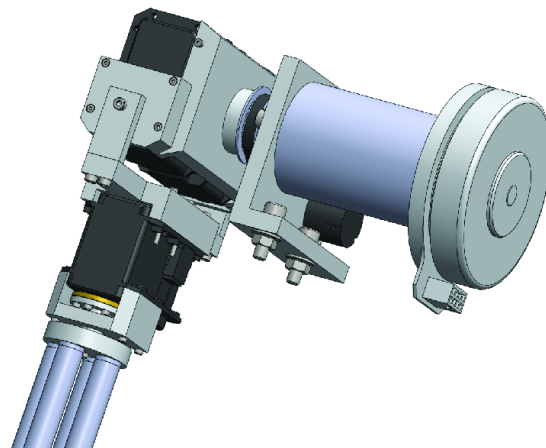




**Luís Filipe Pereira
Almeida Santos**

**Projeto de um manipulador antropomórfico para o
robô CAMBADA@Home**

**Project of an Anthropomorphic manipulator for the
CAMBADA@Home robot**





**Luís Filipe Pereira
Almeida Santos**

**Projeto de um manipulador antropomórfico para o
robô CMBADA@Home**

**Project of an Anthropomorphic manipulator for the
CMBADA@Home robot**

Dissertação apresentada à Universidade de Aveiro para cumprimento dos requisitos necessários à obtenção do grau de Mestre em Engenharia Electrónica e Telecomunicações, realizada sob a orientação científica de Manuel Bernardo Salvador Cunha e José Luís Costa Pinto de Azevedo, professores auxiliares do Departamento de Electrónica, Telecomunicações e Informática da Universidade de Aveiro

o júri / the jury

presidente / president

Filipe Miguel Teixeira Pereira da Silva

Professor Auxiliar da Universidade de Aveiro (por delegação da Reitora da Universidade de Aveiro)

vogais / examiners committee

Manuel Bernardo Salvador Cunha

Professor Auxiliar da Universidade de Aveiro (orientador)

Paulo José Cerqueira Gomes da Costa

Professor Auxiliar da Faculdade de Engenharia da Universidade do Porto (Arguente externo)

**agradecimentos /
acknowledgements**

É com grande estima que quero agradecer aos meus pais, Luís Carlos e Maria Laurinda, por todo o apoio que me concederam para que todo este trabalho tivesse êxito. Por outro lado estou profundamente grato aos professores Manuel Bernardo Salvador Cunha e José Luís Costa Pinto de Azevedo, que me integraram na área dos sistemas robóticos e desempenharam um papel preponderante no desenrolar deste projeto, levantando discussões sempre pertinentes e orientando-me da forma mais viável. Por último mas não menos importantes, quero agradecer aos meus colegas de laboratório João Miranda e Leandro Ferreira por todas as sugestões e contribuições, bem como pela sua camaradagem.

*"Failure is simply the opportunity to begin again,
this time more intelligently."*

— Henry Ford

Resumo

Os robôs de serviço são actualmente um atrativo que tem movido vários investigadores e consequentemente unidades de investigação, tanto privadas como públicas, sendo um bom exemplo deste facto inúmeras Universidades. A competição RoboCup, nomeadamente a sua liga RoboCup@Home, catapulta para a ribalta variados e excelentes projectos, sendo deveras uma montra no estado da arte actual neste tipo de robôs.

Os robôs de serviço têm inúmeras aplicações, desde servir alguém por lazer até apoiar indivíduos não totalmente independentes nas suas tarefas diárias, sem esquecer tarefas morosas e repetitivas que normalmente os seres humanos não gostam de executar.

Neste âmbito, o Grupo de Actividade Transversal em Robótica Inteligente (ATRI) do Instituto de Engenharia Electrónica e Telemática de Aveiro (IEETA), pretende munir o seu robô CMBADA@Home de um braço antropomórfico, este que permitirá uma interação humano robô mais efectiva. Neste sentido, o robô será capaz de transportar objectos de pequeno porte bem como colocá-los num lugar pré-determinado sem ser esquecida a cooperação com humanos no transporte de cargas mais pesadas bem como a aberturas de portas.

Sendo assim, este documento descreve a concepção de uma estrutura mecânica para o braço antropomórfico bem como o desenvolvimento da electrónica de baixo nível inerente ao funcionamento do mesmo.

Abstract

Nowadays, service robots are an attractive that moves numerous researchers and hence research units, publics or privates ones, being Universities a good example of this fact.

RoboCup competition, namely its RoboCup@Home league, brings to the fore various and excellent projects, being a storefront of the service robots state of the art.

Service robots have numerous applications, for instance serving someone for leisure, helping someone with reduced mobility or even perform boring tasks.

In this sense, the Transverse Activity on Intelligent Robotics (ATRI) group, part of the Institute of Electronics and Telematics Engineering of Aveiro (IEETA), intends at endowing the CMBADA@Home robot with an anthropomorphic arm. This arm allow a more effective human robot interaction. Thus, the robot will be able to carry some small objects as well as put them in a predetermined place. Furthermore, this anthropomorphic manipulator will enable the robot to carry heavier loads with human cooperation as well as open doors.

Herewith, this document depicts the conception of an anthropomorphic arm mechanical structure as well as the low level electronics developed on behalf of the arm right performance.

Contents

Contents	i
List of Figures	iii
List of Tables	v
Acronyms	vii
1 Introduction	1
1.1 Motivation	1
1.2 Technological Options	2
1.3 Objectives	2
1.4 RoboCup	2
1.4.1 RoboCup@Home League	3
1.5 Document outline	4
2 Robotic arms concepts	7
2.1 Industrial Robotic Arms	7
2.2 Space Missions Robotic Arms	9
2.3 Robotic Arms in RoboCup@Home League	9
2.4 Research Groups Projects	11
2.4.1 ASIMO	12
2.4.2 Care-O-bot 3	12
2.4.3 PR2	13
2.5 State of the Art	13
2.5.1 NimbRo@Home team	13
2.5.2 NimbRo@Home anthropomorphic manipulator	14
2.6 Summary	15
3 CAMBADA@Home Architecture and design of the Anthropomorphic manipulator	17
3.1 Robot Platform	17
3.2 Software Architecture	18
3.3 Vision System	19
3.4 Localization and Navigation	19
3.5 Human-Robot Interaction	20
3.6 Anthropomorphic Manipulator Development	21

3.6.1	Mechanical Requirements	21
3.6.2	CAD Model	21
3.7	Joints Motor Torque study	27
3.7.1	Shoulder Pitch joint	28
3.7.2	Shoulder Roll joint	29
3.7.3	Elbow joint	30
3.8	Summary	32
4	Control Architecture and Implementation	33
4.1	Operational Requirements	33
4.2	Architecture Overview	33
4.2.1	Process Unit	34
4.2.2	Power System	35
4.2.3	Sensors and actuators	36
4.2.4	Communication System	37
4.2.5	Debugging and Programming System	38
4.3	Hardware Implementation	39
4.3.1	Power System	39
4.3.2	Communication Protocols	40
4.3.3	Sensing and Control Board	41
4.4	Software Implementation	41
4.4.1	Microprocessor Initialization	41
4.4.2	FCM8201 Initialization	42
4.4.3	Dynamixel Chain Initialization	42
4.5	Summary	43
5	Experimental Results	45
5.1	Dynamixel actuation	45
5.2	BLDC step response	48
5.3	Summary	50
6	Conclusion and Future Work	53
6.1	Conclusion	53
6.2	Future Work	53
	Bibliography	55
	Appendices	58
A	Control Board Schematics and Layouts	59

List of Figures

1.1	AMIGO robot performing a task in RoboCup 2013	4
2.1	UNIMATE Robotic Arm in General Motors facilities	7
2.2	Four configurations of industrial robotic manipulators	8
2.3	Robotic Arms in space missions	9
2.4	PERA right arm	10
2.5	Neuronics Katana manipulator with 6 DOF	10
2.6	Homemade robotic arms in RoboCup@Home League	11
2.7	Honda's ASIMO robot	12
2.8	Fraunhofer's Care-O-bot 3 robot	12
2.9	Willow Garage's PR2 robot	13
2.10	Cosero and Dynamaid robots	14
2.11	Schematic of the 7 DOF in the anthropomorphic arms	15
2.12	Cosero and Dynamaid Arms	16
2.13	Design of FinRay grippers	16
3.1	CAMBADA@Home robot overview: Real and CAD models	18
3.2	Microsoft Kinect Camera and SICK LMS100 laser range finder	19
3.3	Microphone array framework	20
3.4	Speaker output device	21
3.5	Anthropomorphic proportions	22
3.6	Frame exploded view	23
3.7	Maxon EC-90 and 66:1 Maxon Gearhead (Real and CAD assembly)	23
3.8	Encoder, pulleys and belt assembly	24
3.9	Encoder, pulleys and belt assembly exploded view	25
3.10	CAD assembly and electrical connections of two MX-106R in synchronous mode	25
3.11	Right Side view and front side view of mechanical interface between MX-106R and carbon fiber pipes	25
3.12	Elbow and wrist yaw joints	26
3.13	Wrist roll and pitch joints	26
3.14	Festo Finray finger and a three Festo Finray grasp	27
3.15	Final mechanical structure of the anthropomorphic arm	27
3.16	Angular displacement <i>versus</i> time	28
3.17	Motor torque produced shoulder pitch joint with no load	29
3.18	Motor torque produced on shoulder pitch joint when the arm is loaded with 1Kg on its hand	29

3.19	Motor torque produced shoulder roll joint with no load	30
3.20	Motor torque produced on shoulder roll joint when the arm is loaded with 1Kg on its hand	30
3.21	Motor torque produced elbow joint with no load	31
3.22	Motor torque produced on elbow joint when the arm is loaded with 1Kg on its hand	31
3.23	Motor torque produced on elbow joint when the arm is loaded with 0.7Kg on its hand	32
4.1	Block Diagram of robot CAN network	34
4.2	Architecture Overview of the Developed Unit	34
4.3	Exploded view of AEAT-6012 mechanical assembly	37
4.4	Close up of separated grounds between power signals and logical signals . . .	39
4.5	Communication architecture overview	40
4.6	Close up of μC connections in sensing and control board	42
4.7	Flowchart of the developed software main functions	43
5.1	Transmitted messages at different baud rates and different return status delay	46
5.2	Total duration of transmitting a message at 57600 bps	47
5.3	Actuating in Dynamixel servos with Write plus Action approach	47
5.4	Actuating in Dynamixel servos with Synchronous approach	48
5.5	Setup assembled for tests	50
5.6	Step responses for 45 degrees displacement	50
5.7	Step response for 90 degrees displacement	51
5.8	Step response for 180 degrees displacement	51
A.1	Final Control Board Schematic - Digital Part	60
A.2	Final Control Board Schematic - Power Part	61
A.3	PCB layout - Top side	62
A.4	PCB layout - Bottom side	62
A.5	First PCB prototype - Top Side	63
A.6	First PCB prototype - Bottom Side	63

List of Tables

2.1	Major differences between Dynamaid and Cosero	14
4.1	Main features of PIC32MX795F512H	35
4.2	Main electric features of Maxon EC-90 Motor	37
4.3	Main features of MX-106R, RX-64 and RX-28 Dynamixel Motors	37

Acronyms

AI Artificial Intelligence. 1, 2

ASR Automatic Speech Recognition. 18

ATRI Transverse Activity on Intelligent Robotics. 1

back EMF back Electromotive Force. 22, 35

BLDC Brushless Direct Current. 2, 29, 31, 33–36, 39, 42, 45, 46

bps bits per second. 12, 31, 34, 41

CAD Computer-aided design. 19–21, 23

CAMBADA Cooperative Autonomous Mobile roBots with Advanced Distributed Architecture. 1, 17, 18, 30, 33

CAN Controlled Area Network. 2, 15, 27, 31, 32, 34, 38

CLK clock. 35

CS chip select. 35

DETI Department of Electronics, Telecommunications and Informatics. 1

DIP Dual In-Line Package. 37

DO data output. 35

DOF Degrees of freedom. 2, 7–12

ERA European Robotic Arm. 7

ESA European Space Agency. 7

HVG High-Voltage Gate. 36

ICD3 In-Circuit Debugger 3. 32, 35

IEETA Institute of Electronic and Telematics Engineering of Aveiro. 1

IR Infrared. 9

Li-Po Lithium Polymer. 15, 28, 29, 33, 34

LUTs Look up Tables. 17

LVG Low-Voltage Gate. 36

NASA National Aeronautics and Space Administration. 7

PCB Print Circuit Board. 35, 37

PERA Philips Experimental Robotic Arms. 8

PI Proportional Integral. 48

PID Proportional Integral Derivative. 48

PWM pulse width modulation. 29, 33, 42, 43, 45, 46

RoboCup Robot World Cup. 1–3

ROS Robot Operating System. 16–18

RTDB Real-Time DataBase. 16

SCARA Selective Compliant Articulated Robot for Assembly. 6

SCK serial clock. 31, 34, 35

SDI serial data in. 31, 35

SDO serial data out. 31, 35

SLAM Simultaneous localization and mapping. 17

SMD's Surface-mount Devices. 37

SPI Serial Peripheral Interface. 31–35, 38, 42, 43

SRMS Shuttle Remote Manipulator System. 7

SS slave select. 31, 34, 35

TQFP Thin Quad Flat Pack. 32

TTS Text-to-Speech. 18

UART Universal asynchronous receiver/transmitter. 31, 38

USB Universal Serial Bus. 31, 35

Chapter 1

Introduction

The year 1997 will be remembered as the heyday of robotics and Artificial Intelligence (AI). On May 11 1997, the IBM Deep Blue Computer won a chess match against the world champion, Garry Kasparov. Later, on July 4 1997, the NASA's creation Sojourner landed successfully on the surface of Mars [1]. These were awesome leaps towards a new future, where robotics performs a major role in everyday life.

Nowadays, service robots have an important role in research and development. One of the main goals is to develop a robot that is capable to help and assist people in their homes, performing various and distinctive activities. To achieve that, the robot must have a very good interaction with human beings, including communications skills and capability of moving objects from a place to another. Furthermore, it must have very good capability of mapping spaces, as well as locate itself and navigate in the space previously mapped. To develop such a robot with the basic features aforementioned, it involves people from different areas, from vision to hardware, passing through high level programming and AI.

1.1 Motivation

The CAMBADA¹@Home is the University of Aveiro RoboCup²@Home team. The project started in January 2011 within the Transverse Activity on Intelligent Robotics (ATRI), a research group in Institute of Electronic and Telematics Engineering of Aveiro (IEETA), based on past experience acquired from CAMBADA soccer team, which has been in a stable growing [2]. CAMBADA@Home team is formed by students of Department of Electronics, Telecommunications and Informatics (DETI) and researchers from IEETA, both from different areas such as image analysis and processing, artificial intelligence and sensor fusion, to name a few. Since CAMBADA@Home team aims at developing a mobile robot designed to improve the aged citizens quality of life in a real-world household environment [2], it's imperative to have manipulation capabilities. Moreover, this team pretends to compete at the highest level in RoboCup@Home League and, regarding this goal, two anthropomorphic arms is a great asset.

¹Cooperative Autonomous Mobile roBots with Advanced Distributed Architecture (CAMBADA)

²Robot World Cup (RoboCup)

1.2 Technological Options

The mechanical parts that compose the anthropomorphic arm must be capable of support mechanic wear. In this sense, a major feature of these parts is mechanical robustness as well as long intervals of maintenance. Furthermore, state of the art technologies are welcome, as long as their costs are within the fixed budget.

Thus, since actuators are parts with some wear, their choices consists on solutions that can afford the desire endurance and performance. A Maxon Brushless Direct Current (BLDC) motor was chosen for the most strong joint in the anthropomorphic arm. This motor has a gearhead coupled that enables to supply a very large torque, comparing to its size. Furthermore, this type of motors have the main advantage of not have brushes, hence mechanical contacts. This fact represents a major asset in terms of lifetime. On the other hand, Dynamixel servo motors are used in the remaining joints. These servo motors allows a very versatile interface, providing several control options to the user and supplying important information about the state of many variables. Furthermore, these motors have a great relation torque-weight, since in few hundreds grams they can support until 10 Nm.

1.3 Objectives

The aim of this project is to develop an anthropomorphic arm with seven Degrees of freedom (DOF), as many as a human arm. This anthropomorphic arm must be able to grab objects and keep them for a short travel, open bottles, manipulate device interfaces, among others. Furthermore, a tailor-made mechanical infrastructure will be designed to interconnect all different joints. The development of this project can be divided into four stages:

- Familiarization and study of Dynamixel actuators and their intercommunication protocol
- Identification of mechanical design requirements
 - physical model with specific measurements for each segment
 - architectural modeling of the final infrastructure
- Development of dedicated controllers for Dynamixel servos array and Maxon BLDC, including their local software
- Integrate such controllers into Controlled Area Network (CAN) network, already existing in the robot structure

1.4 RoboCup

The first official RoboCup took place in Nagoya, in 1997, with participation of 40 teams and over 5000 spectators. Since then, this international competition has been in constant growing, with innovations every year, making it a major vehicle to promote robotics and AI.

The long-term goal of RoboCup could be mentioned as:

By mid-21st century, a team of fully autonomous humanoid robot soccer players shall win the soccer game, compliant with the official rule of the FIFA, against the winner of the most recent World Cup [1].

Hereupon, there is a technical push on state of the Art to pursuit that dream within 40 years, being necessary technicals breakthrough to achieve that task. Needless to say, this main goal needs to be subdivided in several subgoals, which make RoboCup a formidable and healthy challenge, fostering innovation in robotics, AI and related areas.

Nowadays, there are several competitions in RoboCup, which can be divided in the following leagues [3]:

- RoboCup Junior
 - Dance League
 - Rescue League
 - Soccer League

- RoboCup Rescue
 - Robot League
 - Simulation League
 - Agent Competition
 - Infrastructure Competition

- RoboCup Soccer
 - Humanoid Leagues
 - Kid Size
 - Teen Size
 - Middle Size League
 - Mixed Reality
 - Simulation Leagues
 - 2D Simulation League
 - 3D Simulation League
 - 3D Development League
 - Small Size League
 - Standard Platform League

- RoboCup@Home

Each league has its own approach, thus enabling researchers to identify and work on challenges in different areas such as real-time sensor fusion, learning, multi-agent systems, motor control and many more.

1.4.1 RoboCup@Home League

In 2006, RoboCup@Home league came to light in RoboCup initiative. Its main goal is to foster research and development in useful robotic applications that can be used in everyday life to assist individuals in the real-world. Thus, this league has high relevance for future personal

domestic applications and is considered the largest annual competition for autonomous service robots.

This year, 21 international teams from 3 continents [4] competed in RoboCup@Home League, showing that this is currently one of the strongest growing league in RoboCup. Figure 1.1 shows AMIGO robot performing a task during RoboCup@Home challenge in 2013.



Figure 1.1: AMIGO robot performing a task in RoboCup 2013, adapted from [5]

In order to achieve features of helping and assisting individuals, researchers must concentrate their efforts on several domains such as Human-Robot interaction and cooperation, mapping and navigation, object manipulation, ambient intelligence, among many others.

CAMBADA@Home team debuted in RoboCup@Home League in 2011, a competition held in Istanbul, Turkey. The results were below expectations, nonetheless, the team brought valuable experiences which aided to outline a better future [6]. In 2012, CAMBADA@Home participated once more in RoboCup@Home League, this time held in Mexico City. The efforts of the team were materialized in results, providing valuable insight into the future research direction [7].

1.5 Document outline

The document outline is as follows:

- **Chapter 2:** This chapter presents different roles performed by robotics arms, namely in industry, space missions, commercial service robots and academic projects. Being this dissertation a description of an academic project, this chapter depicts state of the art of the service robots developed in academic environment, all of them participants in RoboCup competition.
- **Chapter 3:** This chapter depicts the overall architecture of the CAMBADA@Home robot, as well as the development of the anthropomorphic manipulator mechanical design. In this sense, chapter 3 shows an overview of the hardware and software architecture of the CAMBADA@Home robot, as well as the way it interacts with human beings. On the other hand, since the mechanical structure of the anthropomorphic arm was developed from scratch, this chapter shows a detailed mechanical construction of this manipulator.

- **Chapter 4:** This chapters describes the architecture of the hardware and software implementations for control the anthropomorphic arm joints low level. In this sense, chapter 4 presents how is made the interface between the process unit and sensors/actuators. This chapter also shows the software flux, namely all initializations needed for a correct function as well as the main loop which aims at controlling the anthropomorphic joints behavior.
- **Chapter 5:** This chapter shows and analyzes the main results obtained during this project as well as the setups created for assess those results.
- **Chapter 6:** This chapter presents several conclusions taking into account the implementation used and describes some considerations to improve this project in a near future.

Chapter 2

Robotic arms concepts

Currently, robotic arms are widely spread worldwide. Their applications are diversified, focused mainly in industry, space missions and, more recently, in citizens service. In 1961, the first robotic arm, UNIMATE, was installed at General Motors, job of Joe F. Engelberger and George C. Devol. The UNIMATE is shown in figure 2.1. This arm weighted about 1800 kilograms and was used to drop some car parts into pools of cooling liquid. This fact contributed, in the long term, to the substitution of manpower by machine power [8]. Hereupon, nowadays robotic arms are present in industry with a wide range of sizes, shapes and configurations, thus allowing a large range of applications, each one with its specific features [9].

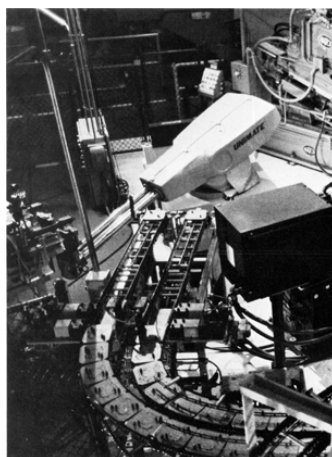


Figure 2.1: UNIMATE Robotic Arm in General Motors facilities, adapted from [10]

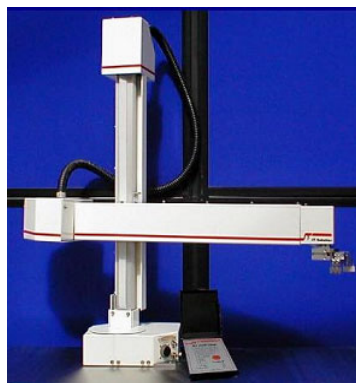
2.1 Industrial Robotic Arms

There are several robot arms mechanical configurations, satisfying different needs and specifications in every industry sector. Among others, the following configurations deserve a particular mention [11]:

- **Cylindrical** Robotic arms with two rotary joints and one prismatic joint. Within its workspace, this arm forms a cylindrical coordinate system.

- **Spherical/Polar** Spherical or Polar arms are identical to cylindrical arms, except for the fact that, in their workspace, they form a spherical coordinate system. Both Cylindrical and Spherical arms have a secondary mission nowadays, performing, mostly, loading and unloading tasks.
- **Selective Compliant Articulated Robot for Assembly (SCARA)** SCARA robotic arms are characterized by their stiffness in vertical direction and compliance in horizontal working plane. Furthermore, due to their parallel form axes, they can easily perform assembly tasks with very high positioning accuracy.
- **Articulated** This configuration of robotic arm has at least three rotary joints and uses weights and springs to counterbalance the relatively long reach and high motor torques. Such a configuration is usually used for spray painting, fettling, gas welding, among many others.

Figure 2.2 shows examples of the aforementioned configurations of robotic arms used in industry.



(a) Cylindrical configuration



(b) Spherical configuration



(c) SCARA configuration

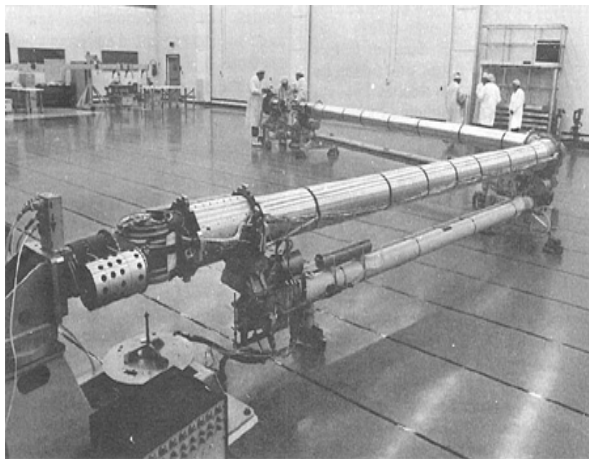


(d) Articulated configuration

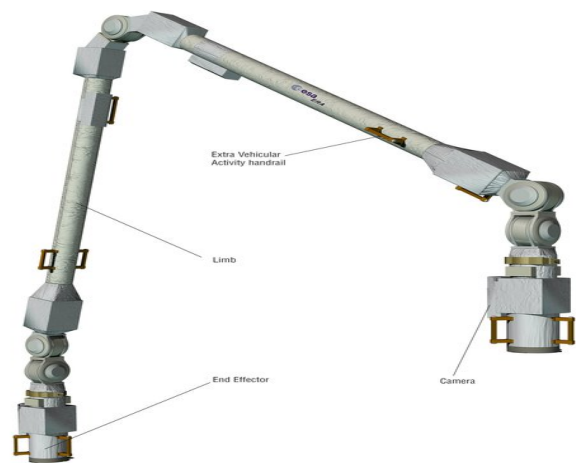
Figure 2.2: Four configurations of industrial robotic manipulators

2.2 Space Missions Robotic Arms

As aforementioned, robotic arms have other applications besides industry. Moreover, robotic arms debuted in industry and then they were adapted and transferred into space missions, services to people, among others [12]. Hence, in November 12, 1981, the Shuttle Remote Manipulator System (SRMS) or Canadarm, shown in figure 2.3a, flew on a Space Shuttle to fulfill a National Aeronautics and Space Administration (NASA) program. This manipulator had 6 DOF and weighed about 410 kilograms, distributed in 15.2 meters [13]. Already in the 21st century, the European Space Agency (ESA) built the European Robotic Arm (ERA), which will be used in partnership with Russian segment of International Space Station. This robotic arm has 7 DOF, measures about 11 meters and weights 630 kilograms [14]. Figure 2.3b depicts ERA manipulator.



(a) Canadarm robotic arm integrated in NASA's Space Shuttle program, adapted from [13]



(b) European Robotic Arm (ERA), leading by Dutch Space (Leiden, The Netherlands), adapted from [14]

Figure 2.3: Robotic Arms in space missions

Although the aforementioned achievements meant great leaps, service robots have played a major role in the robotics research and development, where one can expect that robots will perform dull daily tasks in a real home environment [2]. In this context, RoboCup@Home League instigates teams to improve their robots' features, thus improving the competition level and on the other hand promoting information sharing. Since manipulation is a key issue in RoboCup@Home league, one can find, in that competition, the state of the art in robotic arms.

2.3 Robotic Arms in RoboCup@Home League

Teams in this league have obviously different approaches in their service robots manipulators. Thus, there are teams that build their own new and innovative hardware, while others resort to off-the-shelf hardware in order to focus on algorithmic problems. Moreover, several service robots have just one manipulator and, as opposed, there are teams with two arms service robots. Besides that, one can observe industrial and human-like robotic arms.

The latter one is considered an anthropomorphic arm, since it has human-based shape, 7 DOF, as many as human arm, and an end effector as more possible identical as a human hand.

An example of a commercial robotic arm is Philips Experimental Robotic Arms (PERA), which is used in service robot of Tech United Eindhoven team, AMIGO [15]. AMIGO uses two PERA arms to lift objects up to 1.5 kilograms in each one. PERA has 7 DOF, 3 DOF in shoulder, 1 DOF in elbow, 3 DOF in wrist and weights 3.9 kilograms [16]. Furthermore there are force sensors in each arm joint and an effector, which is comprised by a gripper with a maximum openness of 90 mm. A sketch of PERA right arm is shown in figure 2.4.

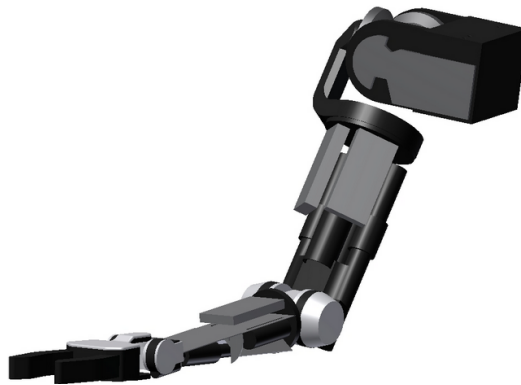


Figure 2.4: PERA right arm [17]

German teams ToBI¹(Team of Bielefeld) and homer@UniKoblenz² also use commercial robotic arms. Both teams equip their service robots with a Neuronics³ Katana manipulator with 6 DOF, which is capable of pick up objects up to 400 grams. This arm has an end effector with 2 DOF, equipped with distance and touch sensors for more accurate grasp [18] [19]. Moreover, Neuronics Katana grants the possibility of different configurations on its effector, which allow different numbers of DOF [20]. Figure 2.5 presents a Neuronics Katana manipulator with 6 DOF.



Figure 2.5: Neuronics Katana manipulator with 6 DOF

¹<http://www.cit-ec.de/ToBI>

²<http://userpages.uni-koblenz.de/~robbie/20/>

³www.neuronics.ch

As aforementioned there are teams which build their own manipulators, for instance WrightEagle@Home team⁴ and Golem⁵ team. They apply in their service robots homemade 5 DOF arm and 3 DOF arm, respectively.

The arm of WrightEagle@Home team has a reach of over 83 centimeters and is able to hold a payload of up to 500 grams while fully extended [21]. The Golem team's manipulator is based on Robotis Dynamixel servos and has a controller to perform default movements such as *park*, *grasp object* and *offer object* [22]. For more accurate grasp, the end effector has Infrared (IR) sensors, which provide distance information for a local object search. Moreover, this arm has a 4th DOF provided by the variation of its height, which is controlled by software [22].

Manipulators described above are depicted in figure 2.6.



(a) WrightEagle@Home team manipulator



(b) Golem team manipulator

Figure 2.6: Homemade robotic arms in RoboCup@Home League

2.4 Research Groups Projects

In addition to academies' research and development groups, nowadays there are several private companies that dedicate their efforts to develop care robots. Certainly, the service robots of tomorrow will be shaped by the results and insights obtained today by those research teams [2]. The following three robots deserve a particular mention.

⁴<http://wrighteagle.org/en/robocup/atHome>

⁵<http://golem.iimas.unam.mx/home.php?lang=es&sec=home>

2.4.1 ASIMO

The Honda's ASIMO robot is the most advanced service robot ever made. It is a legged robot and has a total of 57 DOF. ASIMO was designed to be an all-purpose robot and is capable to perform several chores such as deliver goods, push a trolley as well as run or even kick a ball. This humanoid robot owns a 7 DOF arm, with a hand that has an amazing 13 DOF [23]. Figure 2.7 shows the ASIMO robot, where one can see the human-like shape of the entire body, as well as the robot's arm and hands, endowed of several DOF to fulfill even the most thorough task.

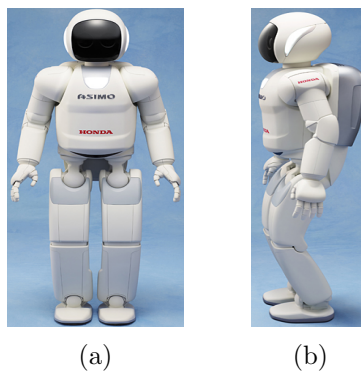


Figure 2.7: a) ASIMO's front view b) ASIMO's side view

2.4.2 Care-O-bot 3

The service robot Care-O-bot 3 is an initiative of Fraunhofer Institute for Production Technology and Automation with the major goal of making a high-tech research platform for development of care robots. This robot has as simple and modular hardware, hence each component can be operated independently by making simple connections. Care-O-bot 3 is equipped with only one 7 DOF light-weight arm (Schunk⁶ LWA 3) and a 7 DOF gripper (Schunk SDH) with tactile sensors [24]. The two latter features make this platform capable of fulfilling tasks such as hand out beverages and open doors. Figure 2.8 presents Care-O-bot robot.



Figure 2.8: Fraunhofer's Care-O-bot 3 robot, adapted from [25]

⁶<http://mobile.schunk-microsite.com/en/produkte/produkte.html>

2.4.3 PR2

PR2 is a robotics research and development platform built by Willow Garage⁷ and aims at assisting and work with people in offices and similar institutional settings. This robot owns a great autonomy, since it can plug-in itself to electrical outlets to charge its batteries. It can also fetch goods from a refrigerator and carry them to a person, as well as open doors [26]. PR2 robot has two manipulators, each one with payload of 1.8 kilograms and 8 DOF in total; 4 DOF in the upper arm, 3 DOF in the wrist and 1 DOF in the gripper. Moreover, the arm owns passive spring counterbalance and powerful wrist and gripper, 4 Nm of torque and 80 N of force, respectively, enabling to grasp and manipulate several objects in everyday life [27]. Figure 2.9 presents PR2 and a close-up of its arm.

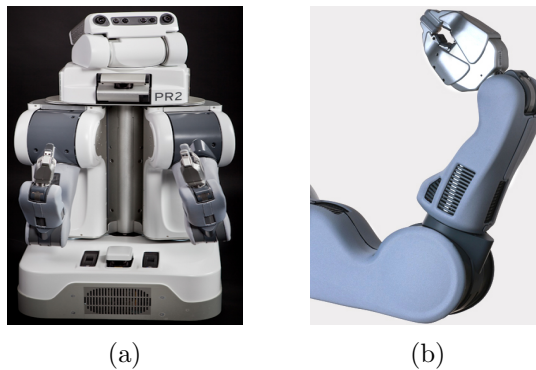


Figure 2.9: a) PR2 overview b) PR2 Arm close up

2.5 State of the Art

The development of an anthropomorphic manipulator portrayed in this document does not pretend to be inserted on a commercial platform but, instead, on an academic project, which can aid the research and development in service robots. Therefore, several academic projects can be considered as a good bottom line, for instance anthropomorphic arms that exist in RoboCup@Home league, many of them described in 2.3.

2.5.1 NimbRo@Home team

The NimbRo@Home is a remarkable team competing in RoboCup@Home League, since it conquered the last three editions of this competition (2011, 2012 and 2013). This academic team from Rheinische Friedrich-Wilhelms-Universität of Bonn owns two self-constructed humanoid robots named Cosero and Dynamaid. These two service robots are comprised of lightweight aluminum parts, which allows a lightweight and inexpensive final construction. Cosero and Dynamaid have omnidirectional drives, enabling them to maneuver in narrow spaces that may exist in real world household environments. Furthermore, a yaw joint in the torso and a linear actuator in the trunk increase the final workspace of the robots. Moreover, the linear actuator is able to move the upper body vertically by approximately 90 centimeters, resembling average human body proportions and reaching capabilities [28]. Both Cosero and

⁷<http://www.willowgarage.com/>

Dynamaid have all joints driven by Robotis Dynamixel actuators. However compared to its predecessor, Cosero has an improved construction and appearance, is more precise and has stronger actuators. Figure 2.10 presents Cosero and Dynamaid robots, respectively, and the table 2.1 depict the major differences between both.

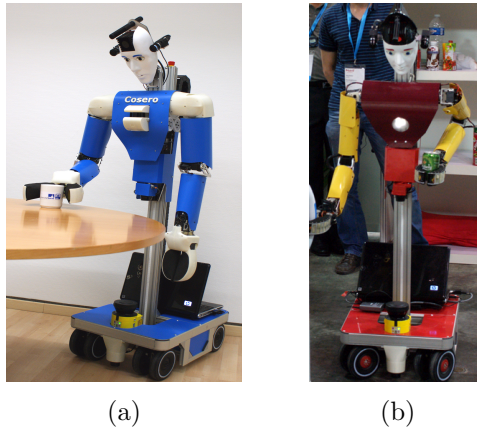


Figure 2.10: a) Cosero service robot b) Dynamaid service robot

	Dynamaid	Cosero
Arm payload	1 Kg	1,5 Kg
Max. Speed	0,5 m/s	0,6 m/s
Weight	20 Kg	32 Kg
Base Size	60 x 42 cm	59 x 44 cm

Table 2.1: Major differences between Dynamaid and Cosero

Since CAMBADA@Home team aims at being on forefront of research and development on service robots, the implementation of an anthropomorphic arm for this team was based on the structure of Nimbro@Home’s anthropomorphic arms, with several adaptations and transformations. Mechanical and electrical design of Cosero’s and Dynamaid’s anthropomorphic manipulators are presented right after.

2.5.2 Nimbro@Home anthropomorphic manipulator

As aforementioned in 2.5.1, all joints of Cosero and Dynamaid are driven by Robotis Dynamixel actuators, which, in electrical terms, communicate bidirectionally via a RS-485 serial bus at baud rates between 9600 bits per second (bps) and 1 Mbps. In this specific case, communication between the robot’s main computer and Dynamixel network is performed by an Atmel Atmega128 microcontroller, at 1 Mbps. In this sense, the main computer communicates over a 1 Mbps RS-232 serial connection with Atmega128 which, on its turn, communicates via RS-485 serial bus with the Dynamixel network.

Dynamaid’s anthropomorphic arm is comprised by 10 Dynamixel actuators, including the gripper. According to the schematic of the 7 DOF in the anthropomorphic arms shown in figure 2.11, the strongest joint in a robot arm is the shoulder pitch joint. This joint is driven by 2 Dynamixel EX-106 in synchronous mode to reach 20 Nm of holding torque (10 Nm in

each other) and rotational speed of 2,3 rad/s. From trunk to gripper, the next three joints are shoulder roll, shoulder yaw and elbow pitch, all of them controlled by single Dynamixel EX-106 servos. Furthermore, the wrist is formed by RX-64 actuators in both yaw and pitch joints and a Dynamixel RX-28 in the wrist roll joint, which are able to stand a 6,4 Nm and a 3,8 Nm holding torque, respectively [29]. Finally, the end effector is composed of two Festo⁸ FinGripper fingers, driven by two RX-28 Dynamixel actuators.

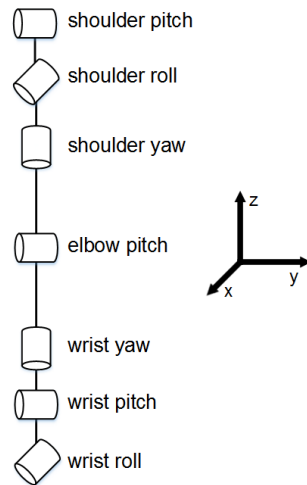


Figure 2.11: Schematic of the 7 DOF in the anthropomorphic arms

On the other hand, as mentioned in the subsection above, Cosero has more accurate and stronger actuators. This fact is in part due to the use of two EX-106+ Dynamixel servos, followed by a 2:1 transduction in the shoulder pitch joint of each Cosero's anthropomorphic arm. Thus, this joint has an holding torque of 42,8 Nm since each EX-106+ owns a 10,7 Nm holding torque [30]. There are also modifications in the wrist joint because the Festo FinGripper fingers in Cosero robot are actuated by two RX-64 Dynamixel actuators. These fingers are made from lightweight plastic material and have the particularity of adapting their shape to the object surface. Therefore the contact surface between fingers and object is significantly extended [31]. Figures 2.12a and 2.12b show Cosero and Dynamaid arms. On the other hand, figure 2.13 depicts the design of FinRay grippers.

2.6 Summary

This chapter presents the history of robotic arms, as well as their application in industry, space missions and service robots, both in commercial and academic branches. Since the project depicted in this document is an academic project, RoboCup@Home represents a case of study. Obviously the off-the-shelf implementations reduces the development time. However the knowledge that can be acquired developing a system from scratch is much more attractive. Moreover, that latter approach results in a system that certainly fits better the user needs.

Finally, anthropomorphic arms of NimbRo@Home team were described since they represent the state of the art of homemade anthropomorphic manipulators, helping the team to win the last three editions of RoboCup@Home league.

⁸<http://www.festo.com/net/startpage/>



(a)



(b)

Figure 2.12: a) Cosero anthropomorphic arm b) Dynamaid anthropomorphic arm [32]



Figure 2.13: Design of FinRay grippers, adapted from [31]

Chapter 3

CAMBADA@Home Architecture and design of the Anthropomorphic manipulator

3.1 Robot Platform

In the beginning of the CAMBADA@Home project, the robot platform was based on the CAMBADA robotic soccer platform with the omnidirectional camera replaced by a low-cost sensor, a Microsoft Kinect depth camera, on the top layer of this platform. In 2012 this platform gave way to a brand new platform which was totally designed and built by ATRI researchers.

Nowadays the CAMBADA@Home robot is composed of a three layer platform which can accommodate in an effective way the number and type of sensors and actuators needed to perform the RoboCup@Home challenges.

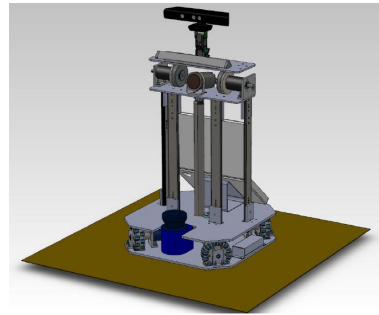
Bottom layer owns a stable and versatile motion solution of four motor system, which drives a symmetrical set of omni-wheels. Moreover, this layer also contains three 4 cells Lithium Polymer (Li-Po) batteries, a SICK LMS100 laser range finder, a support for a linear actuator and the low level control hardware, since the robot adopts a distributed architecture over a CAN network. This bottom layer forms a sandwich like mechanical structure, whose top is used to carry a standard laptop. With this approach, the robot's center of the gravity lowers, increasing the overall stability.

The torso of the robot is represented by a second layer, whose height is variable, i.e., the robot is 0.95 m high in lowest position, while in higher position it reaches 1.40 m, thanks to the linear aforementioned actuator. This layer also contains a speaker and a Voice Tracker II multidirectional microphone array allowing Human-Robot Interaction by voice. Moreover the torso will include a set of two Maxon BLDC motors that will support two anthropomorphic manipulators, whose development is discussed in this dissertation.

Finally, the third layer symbolically represents the head of the robot and in the future will have a set of small programmable oLed screens together with a carbon fiber encapsulation, allowing the creation of dynamic facial expressions. Nowadays, this layer is composed of a pan and tilt structure that holds a Microsoft Kinect depth camera and is also prepared to hold a thermal video camera. Figure 3.1 shows the CAMBADA@Home robot overview.



(a)



(b)

Figure 3.1: a) Real CAMBADA@Home robot b) CAD Model of CAMBADA@Home robot

3.2 Software Architecture

On its debut, CAMBADA@Home team adopted the CAMBADA robotic soccer team general software architecture. This implementation used a distributed approach, which has five different processes executed concurrently - Vision, Agent, Comm, HWComm and Monitor - being the communication between them made by means of a Real-Time DataBase (RTDB) [33].

Nonetheless, the variety of tasks to be performed in @Home league lead to the adoption of Robot Operating System (ROS) as its middleware and framework. This platform has many advantages such as a modular component-driven framework based on the producer/consumer approach as well as an easy integration of third-party code enabling the reuse of well-established solutions. Moreover, the ROS software engineering design provides a variety of tools that encourage faster development.

Although ROS platform provides nodes that fit the needs of the team, CAMBADA@Home is actively developing their own solutions, such as localization and navigation techniques, human-aware robotics, multimodal human-robot interaction and robotic learning [6].

3.3 Vision System

In order to overcome many of the disadvantages inherent to each type of camera, for instance changes in lighting conditions, the CAMBADA@Home robot uses two types of images: color image and depth images. Both images are provided by Microsoft Kinect camera.

The depth sensor of Microsoft Kinect is used to improve the occupation map of the environment, so that being used later to obstacle detection, in association with laser range finder. Moreover, by creating a correspondence between the depth image and the color image, it is possible to add color to the point cloud drawn from the depth sensor alone. Figure 3.2 shows the mechanical assembly of Microsoft Kinect Camera and SICK LMS100 laser range finder in the CAMBADA@Home robot.

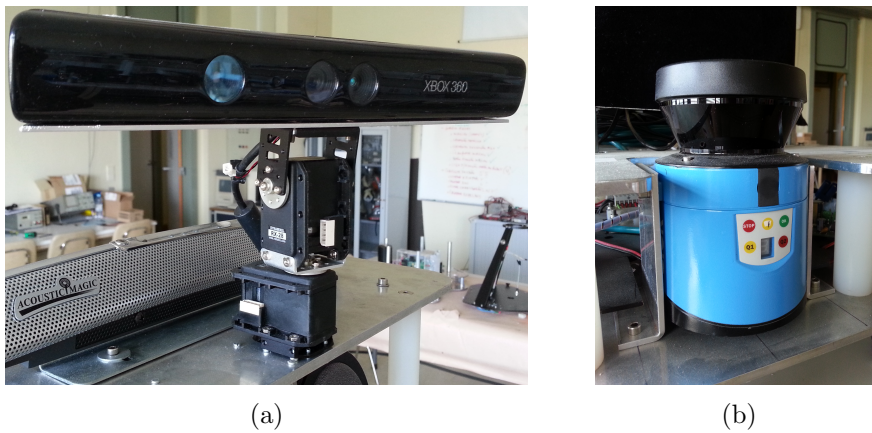


Figure 3.2: a) Microsoft Kinect camera b) SICK LMS100 laser range finder

The object detection is another subject inherent to vision system, regarding the ability to recognize new objects, preferably on-line, and to detect them. This feature can be achieved by segmentation method based in brightness discontinuity and depth, which is used to detect/extract individual objects from an image, and the segmented objects are classified and matched with the proper category by means of feature extraction followed by classifiers.

On the other hand, in order to complete many of the challenges presented in RoboCup@Home competition and also fostering research in the area of Human Robot Interaction (HRI), several algorithms to detect, identify and track humans are under development. For this purpose operations such as analysis of the depth image histogram, segmentation and comparison by shaping matching are performed with the view of detect human and non-human objects. The identification of a person is made by infrared images techniques and in case of success the robot is able to tack her or his movements. Therefore, the Xenics GOBI Longwavelength infrared camera (LWIR) will be used for that purposes.

3.4 Localization and Navigation

The indoor localization in CAMBADA@Home team was successful adopted and adapted from CAMBADA soccer team. This implementation fell back on utilization of Look up Tables (LUTs), which represent the soccer field, and merge their information with vision data. However, with the adoption of ROS platform, the Gmapping node become a powerful

tool to build a map of the environment, using Simultaneous localization and mapping (SLAM) to combine laser scans and odometry information. With this new implementation there is no need of hand measure the environment, since the mobile service robot can perform that chore by itself. Hereupon, the Adaptive Monte-Carlo localization algorithm, another ROS node available, is an useful appliance to localization issues, since it is a well established solution. Although aforementioned solutions are robust and easy to use, the CAMBADA@Home team is evaluating a gradient descent matching between the observed laser scan and the known map of the environment. Actually, this method is used in the Middle Size League CAMBADA team.

Finally, the team is actively researching exploration methodologies, being their intent to research and develop high level navigation techniques using a semantic view in an indoor environment. Therefore, the robot should be able to autonomously build its semantic view in order to accomplish high level navigation tasks, which include for instance reason about its goal and plan the shortest path to that goal.

3.5 Human-Robot Interaction

The Human-Robot Interaction performs a major role in CAMBADA@Home mobile service robot, since it is designed to act in household environment, where people is expected to be.

The most intuitive way to control and process this interaction is by spoken language, which is a natural way for humans, whereas there is no need for additional learning as well as speak enable perform other activities once human members are free.

Therefore, CAMBADA@Home team uses an Automatic Speech Recognition (ASR) component, a Text-to-Speech (TTS) component and a semantic framework to control these two components. The first component is accomplished through the use of CMUSphinx, an open source tool from Carnegie Mellon University. On the other hand, the speech synthesis component is the FESTIVAL Speech Synthesis, developed at the Edinburgh University. These two components will be integrated in the Olympus framework, whose implementation as ROS nodes is under development.

Thus, in terms of hardware, the microphone array framework depicted in figure 3.3, with noise reduction and echo cancellation, is used to speech recognition, and the external speaker shown in figure 3.4 is used as the external speech output device [6].



Figure 3.3: Microphone array framework

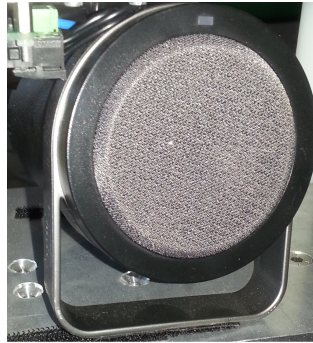


Figure 3.4: Speaker output device

3.6 Anthropomorphic Manipulator Development

As long as the anthropomorphic arm described in this document aims at being used in a service robot, it must obey several constraints, primarily mechanical ones. The following subsections depict such requirements, being these the bottom line for a Computer-aided design (CAD) model for the CAMBADA@Home anthropomorphic manipulator, as well as for its mechanical structure.

3.6.1 Mechanical Requirements

In order to achieve a lifting of small objects such as bottles, small boxes or even garment, it is imperative that the arm structure must move its own weight plus a set payload, which in this project is set between 800 and 1000 grams. With this in mind, the mechanical structure project must consider low weight parts as much as possible, so that the payload can be maximized. Herewith, the upper arm and the forearm are composed of carbon fiber pipes and every home-made component is composed of aluminum, resulting in a robust mechanical structure with low weight. On the other hand the anthropomorphic arm must be capable to put its end-effector on the floor, in the front of the robot, when it is at the lowest position so it can grab objects from the floor. This fact imposes that the final length of the robotic arm, all stretched, is 75 cm. Following the anthropomorphic architecture in the figure 3.5 the upper arm should measure approximately 1,27 more than the forearm.

Beyond these facts, this anthropomorphic manipulator must have a 270 degrees of operation range, starting in full stretched highest position and making 270 degrees in clockwise direction, when the robot is seen by its right profile. This fact comes from human structure, which can perform the same movement. Actually, if the robot wants to perform a task which requests an angle between 270 and 360 degrees of the shoulder pitch joint, this task can be completed by turn the robot around and execute it.

3.6.2 CAD Model

A CAD Model in every mechanical project is a major asset since this leads to a more confident final assembly, saving efforts and resources. Moreover, with a 3D sketch, the project team may vary the final product and test it with different features, searching the best possible construction.

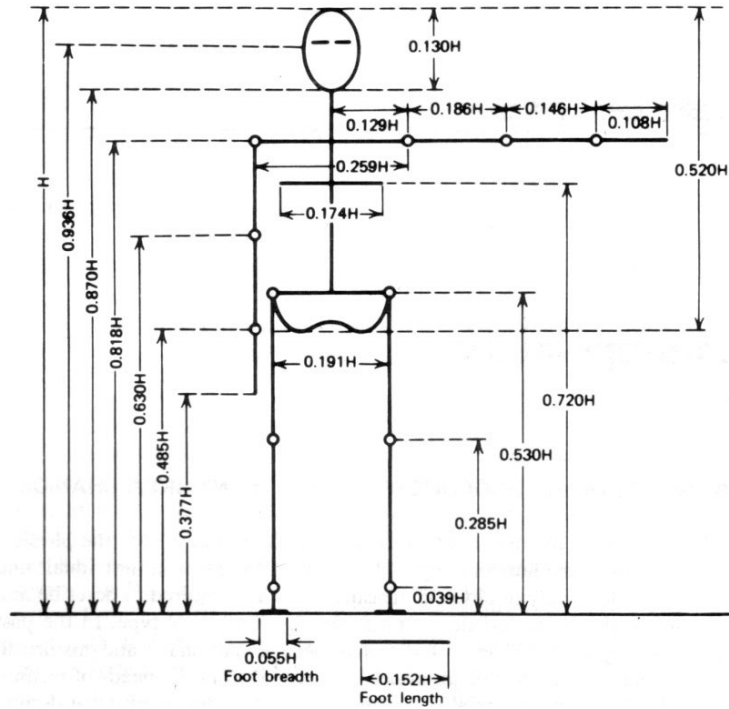


Figure 3.5: Anthropomorphic proportions

In this sense, the CAMBADA@Home anthropomorphic manipulator was designed using a CAD tool, the SolidWorks¹ software, which allows developing the best possible construction that achieves the team goals, as well as a set of very valuable performance tests, narrowing the simulation and reality barrier.

Robotis Dynamixel provide innumerable and distinct frames and horns to enable many assembly configurations, whereby custom and different final assemblies are possible. However, the CAD design for CAMBADA@Home robot, beyond the Dynamixel frames, contemplates custom made aluminum frames which aim at reducing the axial and radial forces at each Dynamixel output shaft bearing.

The reduction of these forces in the Dynamixel output shaft bearing is achieved by a custom aluminum frame, which comprises an extra bearing, helping the Dynamixel inner one. This solution allows a longer life of inner Dynamixel gearboxes, thus becoming the final mechanical structure more reliable. Moreover, all produced torque is mostly delivered to the angular movement, since the inner friction losses are reduced. To achieve this structure, an horn with a shaft is coupled to the original horn provided by Dynamixel, enabling the installation of the outside bearing, which in turn is held by the custom aluminum frame. Figure 3.6 helps to clarify this approach, showing an exploded view of the assembly made by the components mentioned above.

An anthropomorphic arm, as is suggested by its name, is an arm much like a human arm as possible, so the shoulder must be the strongest part of it, since it is the farthest of the end-effector. Hereupon, the shoulder joint must generate enough torque to move a certain payload, considering both the distance from the shoulder to the end-effector and the

¹<http://www.solidworks.com/>

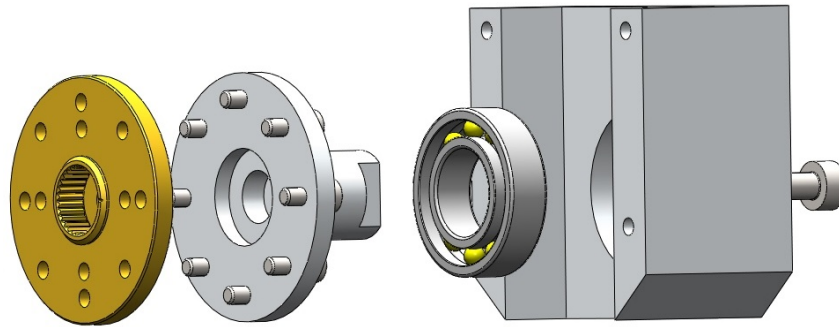


Figure 3.6: Frame exploded view

own arm weight. This fact leads to a choice of a high-torque actuator in anthropomorphic arm first joint, the shoulder pitch joint. Hence, BLDC Maxon EC-90 Motor plus a 66:1 Maxon Planetary Gearhead is used in the first joint, so 28,05 Nm of nominal torque can be debited from its output shaft [34]. Figure 3.7 shows both CAD assembly and real components mentioned above.

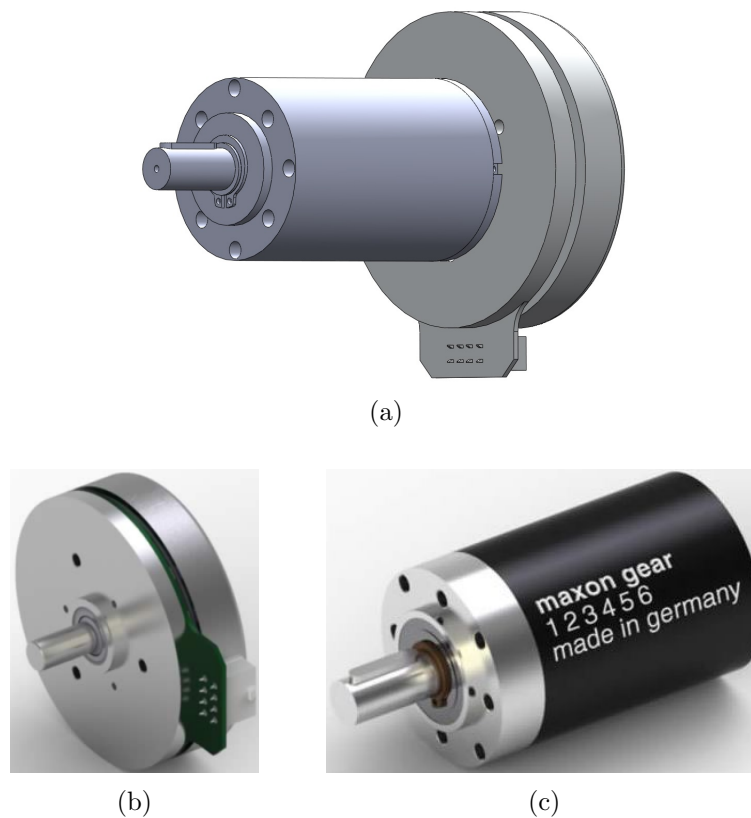


Figure 3.7: a) CAD assembly of Maxon EC-90 with a 66:1 Gearhead b) Real Maxon EC-90 c) Real 66:1 Maxon Planetary Gearhead GP 52

Although the Dynamixel servo motors described below own an associated communication protocol which allows extract many information of it, such as actual position, actual speed,

actual torque and so on, the BLDC Maxon EC-90 Motor does not support this kind of interaction and therefore to know its actual position, for instance, it is necessary to fall back on instantaneous informations from Hall sensors or even back Electromotive Force (back EMF). The handling of results provided by the two methods aforementioned, in order to achieve a consistent result, could be hard to implement as well as request some extra computational effort. Therefore, an absolute encoder is used to collect information about the position of the 66:1 Maxon Planetary Gearhead output shaft, thus allowing its speed to also be assessed. This approach is efficient and easy to use, since the absolute encoder used, the Avago AEAT-6012², uses a series protocol to communicate and its output data is its instantaneous position, with a 12 bits resolution. Note that the position differential and speed of the BLDC Maxon EC-90 Motor is 66 times higher than the 66:1 Maxon Planetary Gearhead output shaft speed.

In order to take advantage of the 12 bits wide, since the shoulder pitch joint only executes 270 degrees, it is necessary use a multiplication principle, which can be obtained by pulleys and belts. In this specific case, the multiplication factor should be $\frac{4}{3}$, i.e., when the arm is in the full stretched highest position the read position should be 0 degrees, as well as after performing 270 degrees the read should be 360 degrees. Hereupon, a pulley concentric with the Gearhead output shaft and a pulley concentric with the encoder output shaft are used, linked with a belt. The relation of $\frac{4}{3}$ could be obtained, at least an approximation, by combining the number of teeth and diameter of the pulleys as well as the belt length. The final assembly of the components aforementioned is depicted in figures 3.8 and 3.9).

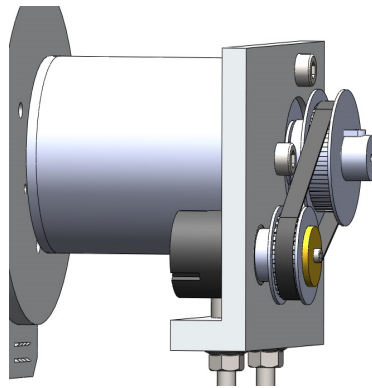


Figure 3.8: Encoder, pulleys and belt assembly

From the first joint on, only Robotis Dynamixel actuators are used, ensuring enough torque for each joint. The second joint, counting from the shoulder on, is responsible for shoulder roll and is composed of two MX-106R Robotis Dynamixel actuators. This 2 servo motors allow a synchronous configuration which enable a 20 Nm nominal torque in shoulder roll joint, since this configuration doubles the available nominal torque at the same angular speed. Figure 3.10 shows the assembly of two MX-106R to provide synchronous features as well as electrical connections to enable that.

The third joint is the shoulder yaw and is composed by a single MX-106R, thus providing 10 Nm of nominal torque as well as 5,76 rad/s of angular speed with no load. Next to this joint, four carbon fiber pipes form the upper arm, which links the yaw shoulder joint to the elbow. This approach, as previously mentioned, allows a strong and lightweight solution to

²<http://partfinder.avagotech.com/Avago/Avago.jsp#!partSearch=&partno=AEAT-6012&pagenum=1>

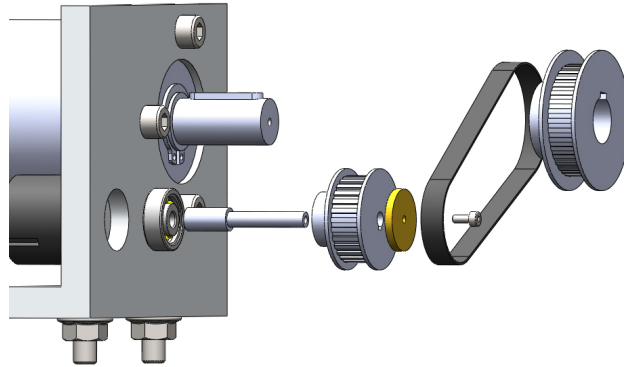
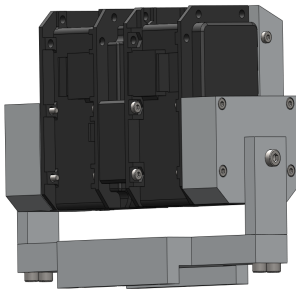


Figure 3.9: Encoder, pulleys and belt assembly exploded view



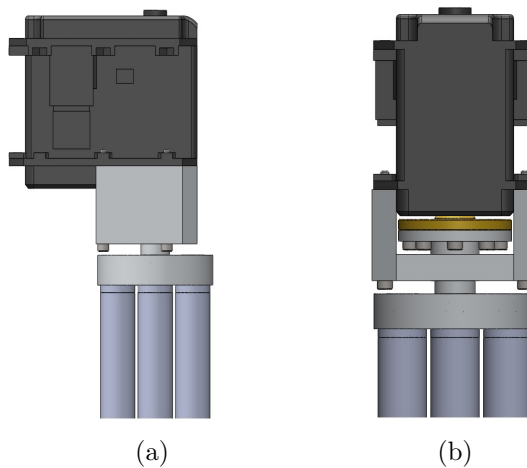
(a)



(b)

Figure 3.10: a) Two MX-106R in synchronous mode assembly b) Electrical connections on synchronous mode, adapted from [35]

link joints in the anthropomorphic arm. Figure 3.11 shows the CAD mechanical interface between the third joint and carbon fiber pipes.



(a)

(b)

Figure 3.11: a) Right view of mechanical interface b) Front view of mechanical interface

The elbow, likewise the shoulder yaw joint, is formed by a single Dynamixel MX-106R, which aims at performing movements like an human elbow. Thus a mechanical structure was developed to allow lifting a payload only moving the elbow.

Wrist yaw joint is effectively the fifth joint, composed of a single Dynamixel RX-64 and assembled next to the elbow, providing a movement much identical as possible as the human one. Note that when an human performs a wrist yaw movement the forearm moves too, so the wrist yaw joint is assembled right after the elbow joint and is proceeded by carbon fiber pipes. Figure 3.12 shows the assembly composed of elbow joint, wrist yaw joint and the carbon fiber pipes which links this fifth joint to the next wrist joints.

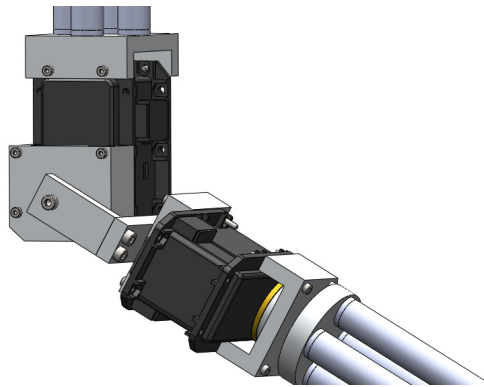


Figure 3.12: Elbow and wrist yaw joints

Right before the end effector, lies the wrist roll and pitch joints, which are composed of RX-64 and RX-28 Dynamixel servos, respectively. These two joints, together with the wrist yaw joint, form a wrist with 3 DOF, allowing total freedom of the end effector for a more accurate and fast grip. Mechanical assembly of the two latter joints is depicted in figure 3.13.

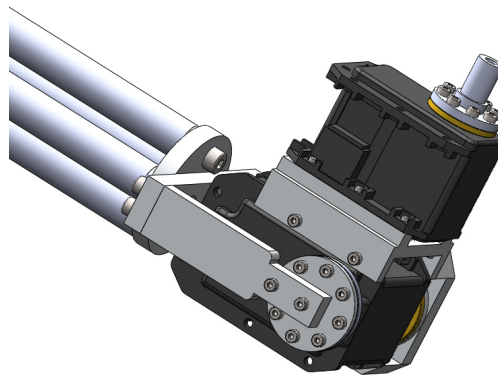


Figure 3.13: Wrist roll and pitch joints

Being out of the scope of this document, and despite the fact of being a major part of an anthropomorphic arm, the end effector can be materialized in many ways, so the grasp could be as better as possible. Hereupon, Festo FinRay fingers approach is an available solution, which represents an high quality grasp in various and different objects, once the mechanical structure is very versatile. This solution presents various models with different dimensions, which can be used for grasp objects with different textures, shapes, sizes and

solidity. Obviously an hand is formed by two or more FinRay fingers, being an utilization of two the best *trade-off* since this solution allows an handling of many objects maintaining an acceptable weight. An example of a FinRay finger as well as a grasp performance are presented in figure 3.14.

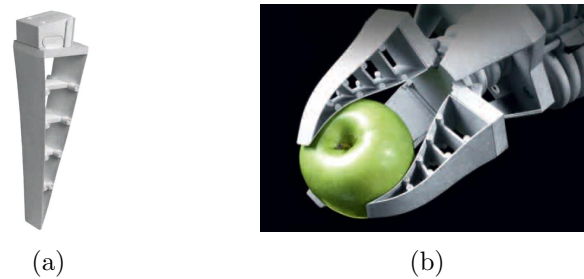


Figure 3.14: a) A Festo Finray finger b) Three Festo Finray fingers grasping an apple. Adapted from [35]

Finally, figure 3.15 depict the entire mechanical structure developed for anthropomorphic manipulator.

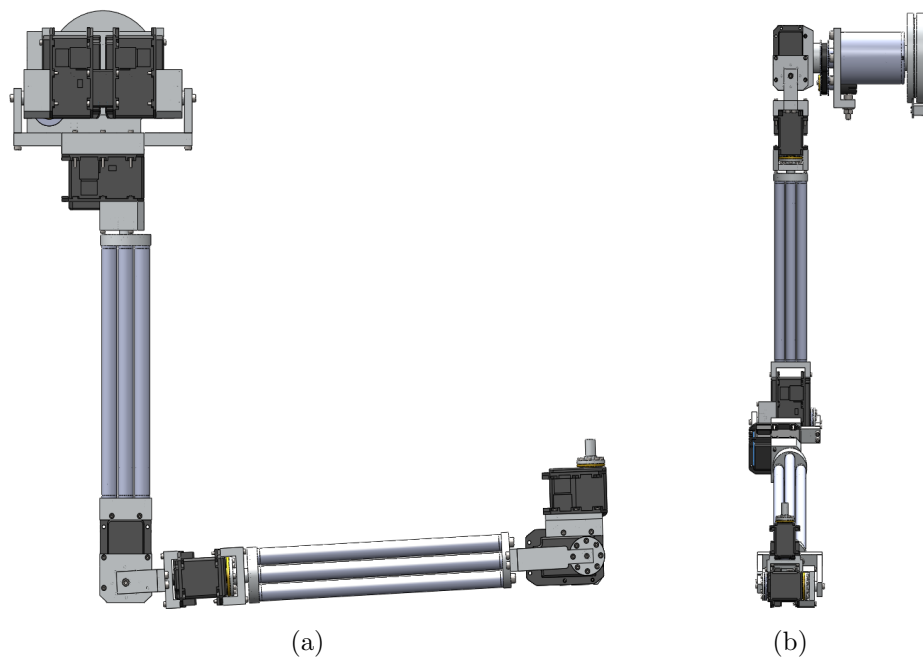


Figure 3.15: a) Left view of the final mechanical structure of the anthropomorphic arm b) Front view of the final mechanical structure of the anthropomorphic arm

3.7 Joints Motor Torque study

This section aims at presenting some results obtained using the tools provided by the CAD software used in this project. Thus, a study of three important joints was realized,

simulating a real movements of the anthropomorphic arm. Furthermore, these simulations took into account the arm without any extra load and the arm with a simulated load.

The joints simulated were shoulder pitch, shoulder roll and elbow joints, all of them moving 90 degrees, starting from the all stretched position of the arm, i.e., when the arm is fully stretched along the robot body and perpendicular to the floor.

Although these simulations could not represent the real conditions of the arm future environment, they could provide relevant data aiming at characterizing the anthropomorphic manipulator.

Figure 3.16 shows the angular displacement of the joints mentioned above during the simulation time.

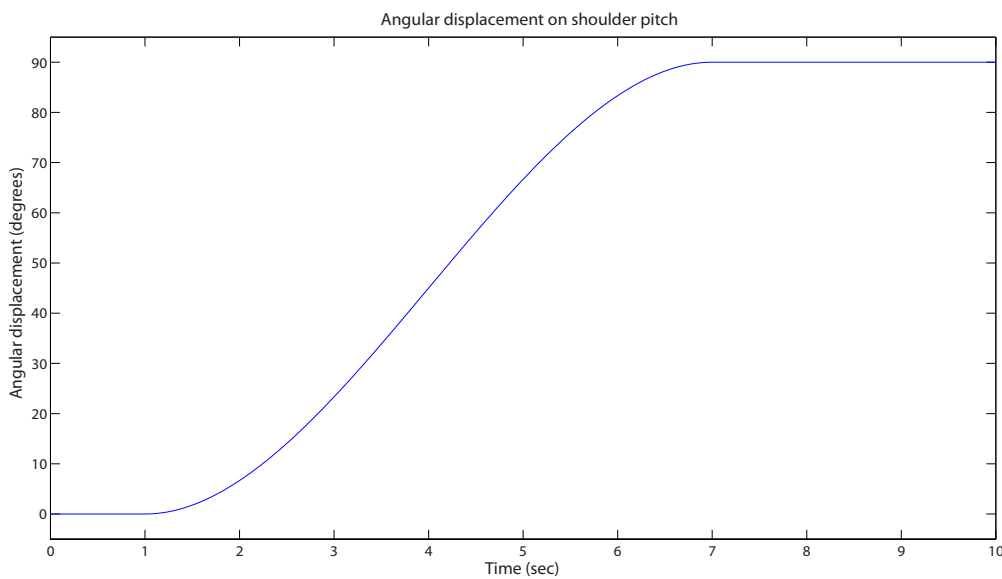


Figure 3.16: Angular displacement *versus* time

3.7.1 Shoulder Pitch joint

The shoulder pitch joint is the most powerful, in terms of torque produced, in the anthropomorphic mechanical structure. This joint must debit a torque capable of moving the entire arm plus an additional load. Figure 3.17 shows the torque produced by the shoulder pitch joint motor when the anthropomorphic arm has not an extra load, i.e., the shoulder pitch joint motor only supplies the torque needed to lift the own weight of the arm. On the other hand, figure 3.18 depict the torque produced when the arm is loaded with 1Kg on its hand.

As one can see, the maximum torque produced is approximately 4,7 Nm and 22 Nm, in case of no load and in case of a load of 1Kg, respectively.

Note that the final torque is necessary to maintain the arm in the final position, in this case fully stretched and parallel to the floor.

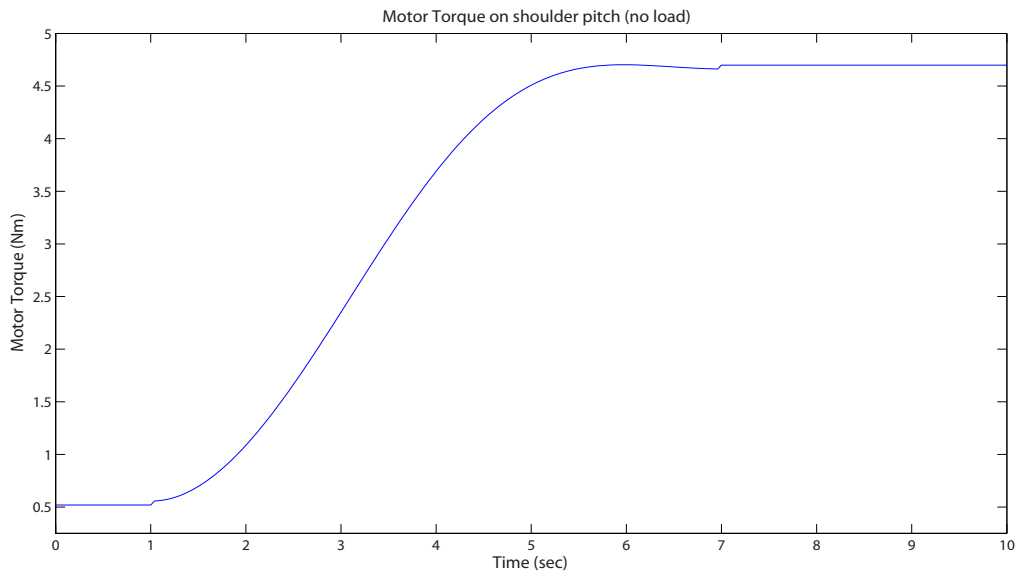


Figure 3.17: Motor torque produced shoulder pitch joint with no load

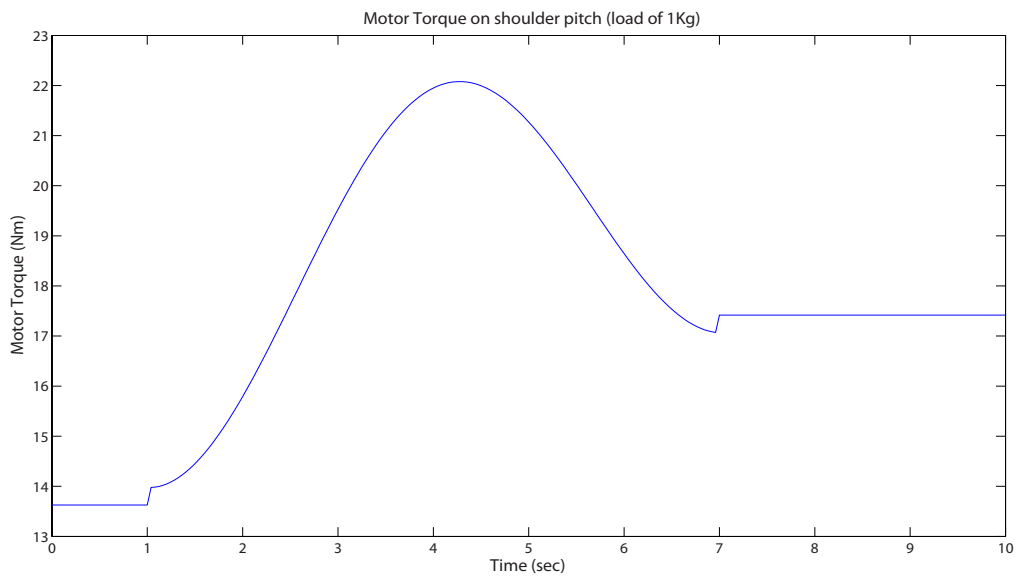


Figure 3.18: Motor torque produced on shoulder pitch joint when the arm is loaded with 1Kg on its hand

3.7.2 Shoulder Roll joint

This joint is composed of two Dynamixel MX-106R, thus it is capable of debit 20 Nm of torque, since each MX-106R can produce 10 Nm. The figure 3.19 depict the torque needed to move the arm in a 90 degrees displacement with no load. It is visible that are necessary a maximum of approximately 4 Nm. On the other hand, when the arm is loaded, the torque needed rises to a maximum of approximately 18 Nm. Figure 3.20 depict this fact.

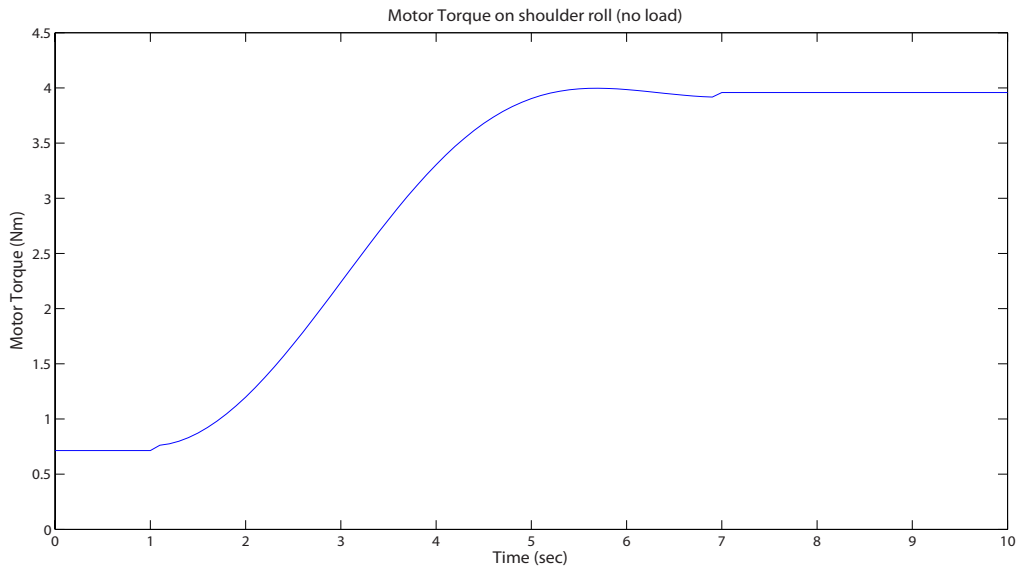


Figure 3.19: Motor torque produced shoulder roll joint with no load

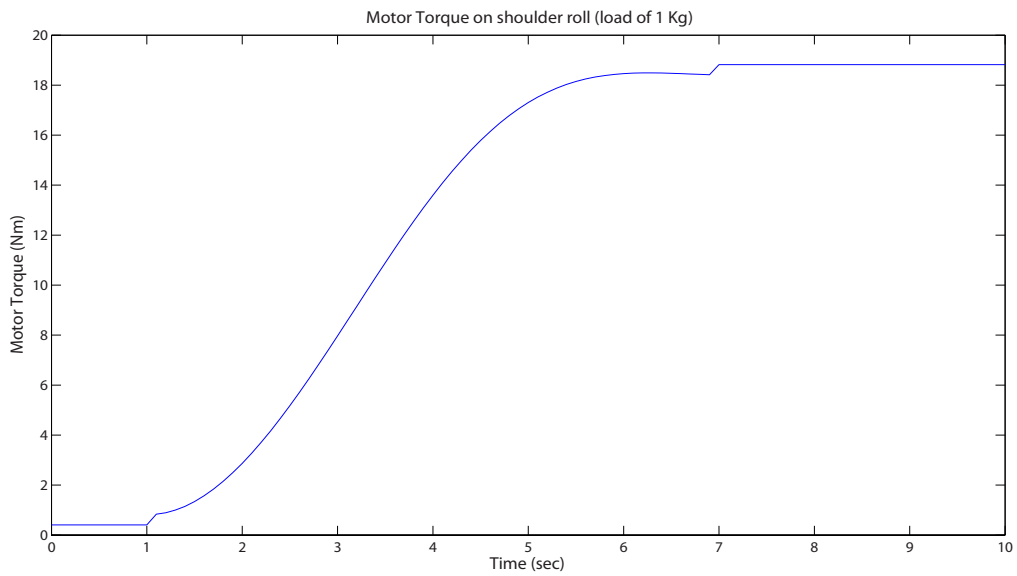


Figure 3.20: Motor torque produced on shoulder roll joint when the arm is loaded with 1Kg on its hand

3.7.3 Elbow joint

The elbow joint is approximately at the middle of the mechanical structure of the anthropomorphic arm. Thus, with a 90 degrees displacement this joint supports the torque needed to lift up the forearm and the wrist. Figure 3.21 represents the torque needed in this joint to move only the remaining weight of the arm, while figure 3.22 depict the torque needed to move remaining weight of the arm plus a simulated load of 1Kg.

As one can see, when the arm is loaded with 1Kg, the torque supplied by the elbow joint

in this movement is approximately 12 Nm. This torque transcends the maximum stall torque of a Dynamixel MX-106R. However, figure 3.23 shows the torque needed on the elbow joint to lift up the remaining weight of the arm plus a load of 700 grams (0.7Kg). As one can see, the torque needed now has a maximum of approximately 8,5 Nm.

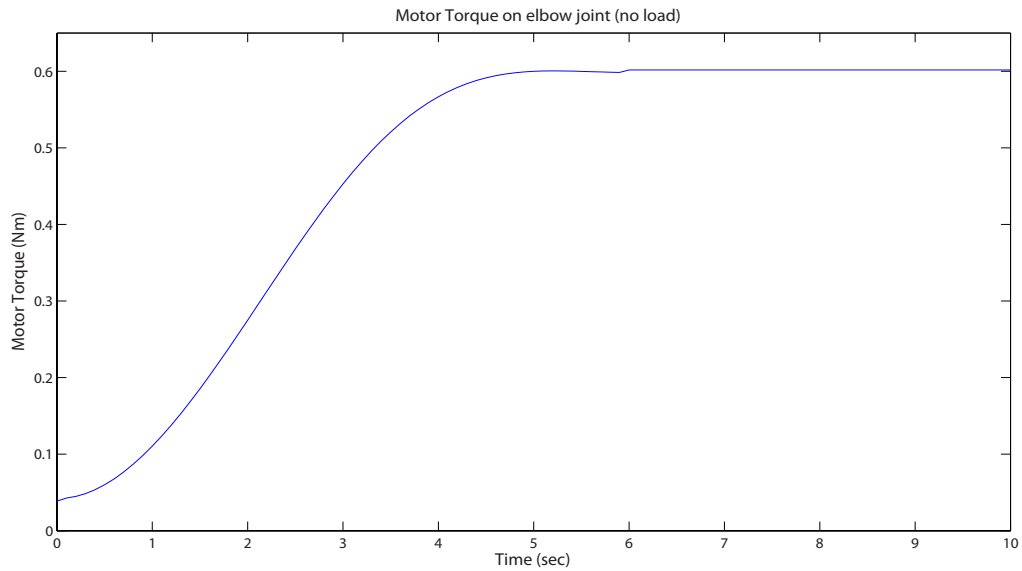


Figure 3.21: Motor torque produced elbow joint with no load

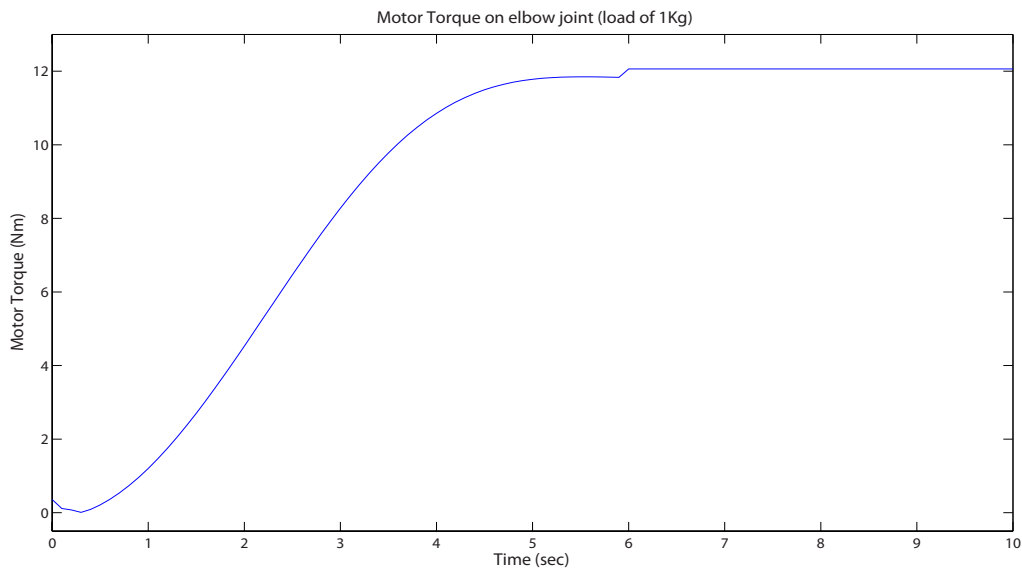


Figure 3.22: Motor torque produced on elbow joint when the arm is loaded with 1Kg on its hand

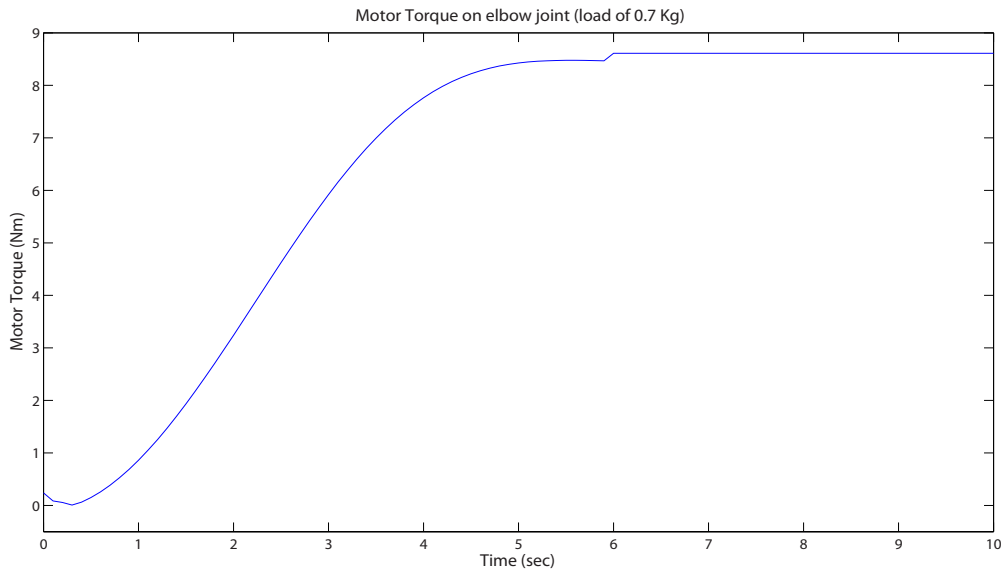


Figure 3.23: Motor torque produced on elbow joint when the arm is loaded with 0.7Kg on its hand

3.8 Summary

This chapter presents the existent overall architecture of the CAMBADA@Home robot as well as the mechanical design of the anthropomorphic manipulator developed, aiming at integration the robot's structure.

Since CAMBADA@Home is a project in progress, its mechanical structure as well as its system architecture in terms of hardware and software, are in permanent changing. In this sense, the robot has been better performances as well as increasingly skills thanks to several researchers efforts. Since the goal of the anthropomorphic manipulator is to be a part of the present mechanical structure of the CAMBADA@Home robot, all dimensions and features have the actual morphology as a bottom line.

Chapter 4

Control Architecture and Implementation

4.1 Operational Requirements

A service robot must have an excellent perception of its environment as well as a capacity of navigation without neglecting the safety of people and objects. Hereupon, the anthropomorphic arm, when touched on something or someone around, should detect the collision and lower the stiffness to avoid damages, as well as inform the system about the occurrence. Moreover, following the functional idea of distributed architecture already implemented, all joints of the anthropomorphic arm must be unified in one process unit, which in turn communicates over the CAN network with the processing unit of the robot. Therefore, every information of a desired movement or every information that the central system wants to collect passes through the low-level control unit, whose implementation is discussed in this Chapter.

Therefore, this control unit must be prepared to receive action information to all joints as well as provide information about all joints which the arm is made of. Since the manipulator solution described in this document implies two types of actuators, Dynamixel servo motors and a Maxon Brushless Motor, the unit depicted in this chapter must be endowed with features to control that, primarily different communication protocols and a proper supply system.

4.2 Architecture Overview

As aforementioned, the anthropomorphic control unit is integrated in the robot architecture by means of a CAN network. In this sense, this is another node integrating the robot CAN network, beyond the already implemented ones: wheel motors with odometry and pan & tilt nodes. The CAN network may be seen as the nervous system of the robot, once its nodes control different low-level sensing/actuation systems and all of them communicate with the processing unit by means of a CAN bus. Figure 4.1 depicts the robot CAN network as well as its nodes, where the manipulator node is also included.

On the other hand, the manipulator node itself must be concerned about the interaction with different devices, coordinating the low level of each one. Figure 4.2 shows the overview of the control unit developed, presenting the peripherals of this project, debugging, supply and process system, as well as the communication protocols used, when applicable.

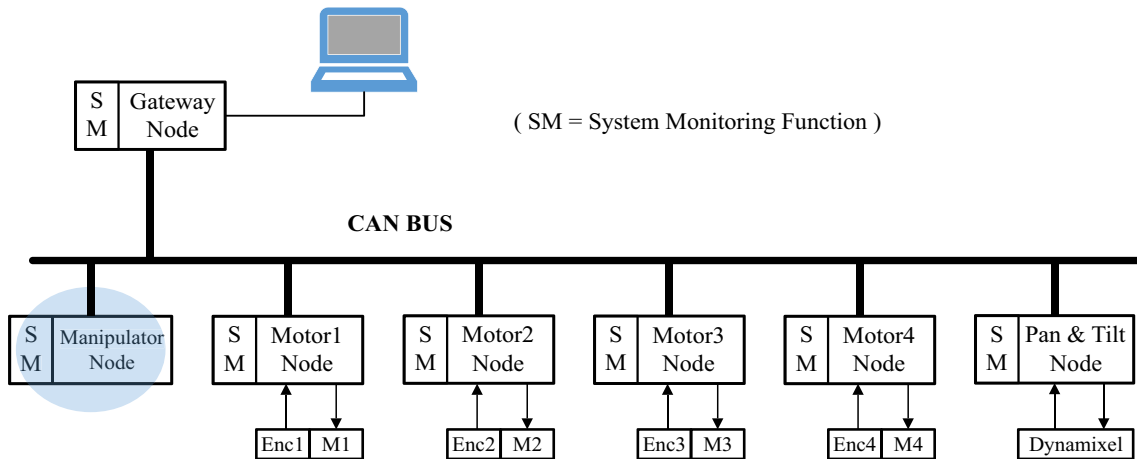


Figure 4.1: Block Diagram of robot CAN network

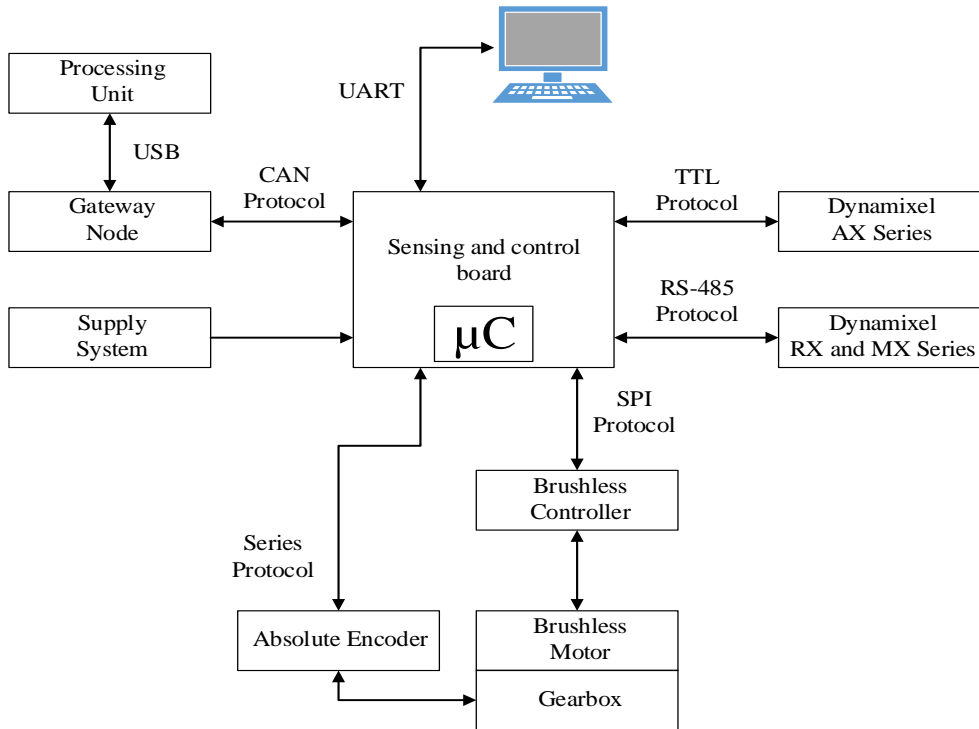


Figure 4.2: Architecture Overview of the Developed Unit

4.2.1 Process Unit

For all facts above mentioned, it is clear that the developed control unit must be endowed with a central controller which is capable of acquire informations from the sensors and act in actuators according to a predefined algorithm. This central process unit must owns a set of features that can be depicted as follows:

- Inner peripherals able to implement CAN protocol and Serial Peripheral Interface (SPI) protocol
- Enough number of UART to deal with implementation of TTL, RS-485 and debugging
- Above average RAM size, which can deal with some low-level calculations
- Low energy consumption, increasing batteries autonomy in a mobile platform

In this sense, once the previous experience of the author lies in Microchip¹ PIC micro controllers (μC), the process unit for this low level platform is the PIC32MX795F512H, whose characteristics and inner peripherals fit the need of this project. Furthermore, this μC presents some packages, including Thin Quad Flat Pack (TQFP), which has a good trade-off between number of pins and size, once this characteristic is important to not oversize the project. Some characteristics of this process unit are shown in table 4.1.

Microchip PIC32MX795F512H	
Operating Voltage Range	2.3V - 3.6V
Maximum Frequency	80 MHz
Flash Memory	512 KB
RAM	128 KB
Timers 16-bit	5
Timers 32-bit	2
UART	6
SPI	3
I ² C	4
CAN Modules	2

Table 4.1: Main features of PIC32MX795F512H [36]

Although this device has a good number of inner peripheral in terms of communication protocols, all of them are shared, i.e., some pins of the μC provide both UART and SPI protocols as well as some pins provide UART and CAN protocols, among others combinations, however can only be used one at a time.

4.2.2 Power System

The most important feature of the developed control unit is its Power System, since without this issue under control all efforts developed can be useless. Like mentioned in section 3.1 the CAMBADA@Home mobile service robot has a power system composed of three batteries of 4 Li-Po cells each. They supply all logical connections as well as power connections, using two fully independent powering circuits, by means of optical isolation, one for the logical parts, and another for the more high energy level power circuits. In order to supply logical circuits, one 4 cells Li-Po battery is used, hence providing 16,8 Volt (when totally charged). On the other hand, to supply wheel motors, which have a nominal voltage of 24 Volt, a series association of two 4 cells Li-Po batteries is used, so providing 33,6 Volt when

¹<http://www.microchip.com/>

totally charged. The energy delivered to the motors is controlled by a pulse width modulation (PWM) approach, aiming at assure the desired speed set-point for each controller.

The operation voltage of Dynamixel servo motors varies according with the series, having a range between 10 and 18,5 Volt. MX-106 series owns a 10 to 14,8 Volt range while RX-28 and RX-64 series have a range between 12 and 18,5 Volt. Furthermore, recommended voltages are 12 and 14,8 Volt, respectively [37][38][39]. Thus, the MX-106 series can not be supplied by 4 cells Li-Po batteries, since their totally charged voltage is 16,8 Volt. Thus, 3 cells Li-Po batteries which present a totally charged voltage of 12.6V fit the conditions. On the other hand, RX-28 and RX-64 series can be supplied by 4 cells Li-Po batteries, once its maximum supported voltage is 18,5 Volt and, as previously mentioned, 4 cells Li-Po batteries owns 16,8 Volt when totally charged.

Besides BLDC Maxon Motor and Dynamixel servo actuators, it is imperative to supply the control electronics. Therefore, there is linear voltage regulators in order to provide the proper voltage, both in logical and power sides. These implementations are described below, on section 4.3.1.

4.2.3 Sensors and actuators

The major components of the project depicted in this document are its actuators and sensors. In this particular project the actuators are all rotative motors, BLDC Maxon EC-90 Motor as well as Dynamixel servo motors. The latter ones have an inner control, which enables to interact in a high level way with the motor itself and assess many variables such as position, speed, torque, temperature, among many others. On the other hand, the EC-90 needs an external controller to provide an efficient supply to its three phases, using to that purpose the same number of Hall sensors, whose combination determines the proper sequence to apply on BLDC phases, aiming at moving the Maxon EC-90 output shaft. In this project is used the integrated circuit FCM8201, by Fairchild, as the BLDC motor controller. To estimate the position and hence the velocity of EC-90 an absolute encoder is used, the Avago AEAT-6012. This device uses a magnetic Hall effect contactless sensing technology to provide absolute angle detection, in this case with 12 bits, hence 0.0879° of resolution. These 12 bits are provided in serial bit stream, which recommended maximum read out frequency is 1 MHz [40]. An exploded view of AEAT-6012 mechanical assembly is shown in figure 4.3, where one can see the magnetic contactless operating principle.

The Maxon EC-90 Motor (EC for electronic commutation) is a 12 pole pair motor, with external rotor and 90 W of nominal power. This motor, being a BLDC, presents drawbacks and benefits relatively to brushed DC motors. BLDC motors have a longer life than brushed ones, however they need a much more complex electronic control. On the other hand, brushed systems limit the motor speed and cause brush spark, generating considerable electromagnetic interferences, while the brushless motors can achieve higher speeds and iron losses can be kept low [41]. Next table (Table 4.2) depict the main electric features of Maxon EC-90 Motor.

The Dynamixel servos motors are spread worldwide, once they have an excellent relation weight-performance, becoming ideal for applications where weight matters and the precision movement at a high torque is fundamental. Herewith, these motors with engineering plastic body and Maxon motors represents a very good solution for this project. There are three different Dynamixel series in use in this project, MX-106R, RX-64 and RX-28, each one with its features, which are present in the next table (Table 4.3).

Although this project does not use Dynamixel AX series actuators, which work based

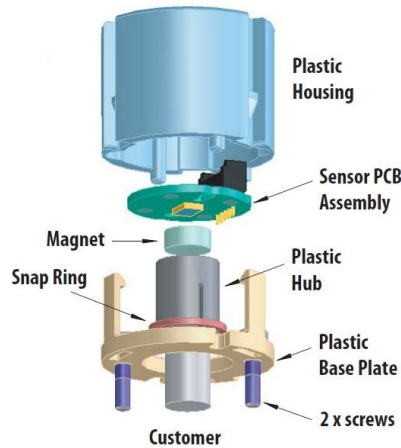


Figure 4.3: Exploded view of AEAT-6012 mechanical assembly, adapted from [40]

Maxon EC-90 Motor	
Nominal Voltage	24 V
Nominal Power	90 W
Nominal Torque	0.425 Nm
Nominal Current	5.84 A
Starting current	70 A

Table 4.2: Main electric features of Maxon EC-90 Motor [34]

	MX-106R	RX-64	RX-28
Recommended Voltage	12V	14.8V	14.8V
No load Speed	45 rpm (@ 12V)	64 rpm (@ 18.5V)	85 rpm (@ 18.5V)
Stall Torque	8.4 Nm (@ 12V, 5.2A)	5.3 Nm (@ 18.5 V, 2.6A)	3.7 Nm (@ 18.5V, 1.9A)
Weight	153 g	125 g	72 g
Protocol Type	RS-485		

Table 4.3: Main features of MX-106R, RX-64 and RX-28 Dynamixel Motors [37][38][39]

on a TTL Level Multi Drop Bus, the author decided to implement such bus, since the CAMBADA@Home is a work in progress, so that Dynamixel AX series could be used in the future.

4.2.4 Communication System

The communication system assures that a data flow is proper delivered to its destination while maintaining the integrity of data. Therefore, the information must be transmitted between components in a language that all stakeholders understand, the communication protocol. These components can be sensors, actuators or even the control unit. Furthermore, sensors and actuators have their own communication protocol and the control unit must implement these protocols to establish communication with them. In this sense, the control unit can communicate with Dynamixel servos through the RS-485 protocol (RX series and beyond) and half duplex asynchronous serial communication protocol (AX series), while

BLDC Motor controller can be accessed by SPI communication protocol. The communication between the absolute encoder and the control unit is achieved by a serial bit stream, which is implemented only by the internally ports of the μC . Furthermore, the control unit also supports the CAN protocol, enabling it to communicate with the process unit of the robot. Between each process unit and every low level control there is a gateway, whose mission is to establish the interface between the low level CAN network and the Universal Serial Bus (USB) connection to the main computer unit.

The SPI protocol is used to access the BLDC controller. This series protocol has 4 connections, serial data out (SDO), serial data in (SDI), slave select (SS) and serial clock (SCK) and, unlike the other protocols described in this document, SPI operates in full-duplex mode. This protocol uses the master/slave approach, being the clock signal headed by the master device, and the slave device is selected by the SS signal. Thus, this configuration allows to have multiple slaves, in case of multiples and individuals SS signals.

The half duplex asynchronous serial communication protocol is implemented physically by a TTL Level Multi Drop Bus, which is configured with 8 data bits, 1 stop bit and no parity. Furthermore, this protocol is based in Half Duplex UART serial communication, where both transmitting and receiving data can not be used at the same time. Therefore, one device is transmitting while all the others need to be in input mode, in order to assess if they are the information addressee. The TTL Level Multi Drop Bus is implemented in this project using a PIC32MX795F512H internal UART as well as a quad buffer MC74LCX125 to control the data flow direction between the bus and the μC .

On the other hand, the RS-485 protocol, which is also another asynchronous serial communication protocol, uses another UART of PIC32MX795F512H to generate data with 8 data bits, 1 stop bit and no parity. However, to implement this physical protocol is necessary to add an external component, the transceiver MAX3362. This device is composed of one differential transceiver, consisting on a line driver and receiver, which allows selecting the data flow direction [42]. Once RS-485 lies on a differential approach, this protocol is physically implemented using a 4 connections bus - VCC, Ground, D^+ and D^- . Furthermore, the μC acts as a master in this approach and the Dynamixel actuators are slaves.

Long last, but not the least, the CAN protocol in the μC is controlled by a CAN module, a PIC32MX795F512H inner peripheral. However, there is a transceiver MAX3051 responsible for physical interface between μC pins and CAN bus lines.

4.2.5 Debugging and Programming System

An important issue on systems developing is the capability of identify erroneous. Therefore, the control unit developed must be capable of receive test orders and send some information about the real state of desired variables of the system. Thus, an Universal asynchronous receiver/transmitter (UART) communication is used aiming at establish a connection with a laptop in order to crate log files, which contain important informations to find potential problems.

On the other hand, In Circuit Debugger 3 (ICD3), by Microchip, is used to debugging any algorithm malfunction on its execution time.

Actually, the debugging system is sometimes forgotten or even underestimated during the project, however some resources of the control unit must be designed to debug the entire system.

Another central importance matter in the control board project is the programming system

used to program and verify an algorithm in the μC , which represents the reasoning of all unit. To perform that chore, it is used a Microchip Tool, the In-Circuit Debugger 3 (ICD3), allowing send to μC the desired software, verify the programming success, halt the μC execution, clear all previous programs, among others features.

4.3 Hardware Implementation

4.3.1 Power System

As aforementioned in 4.2.2, the CAMBADA@Home mobile service robot has logical and power circuits optically separated. Therefore, once this project as a unit to integrate in that robot, this approach must be followed. Thus, it is imperative the use of optocouplers, whose major role is to provide some type of communication between logical side and power side. This communication is achieved by means of SPI protocol. Figure 4.4 helps to understand the facts mentioned.

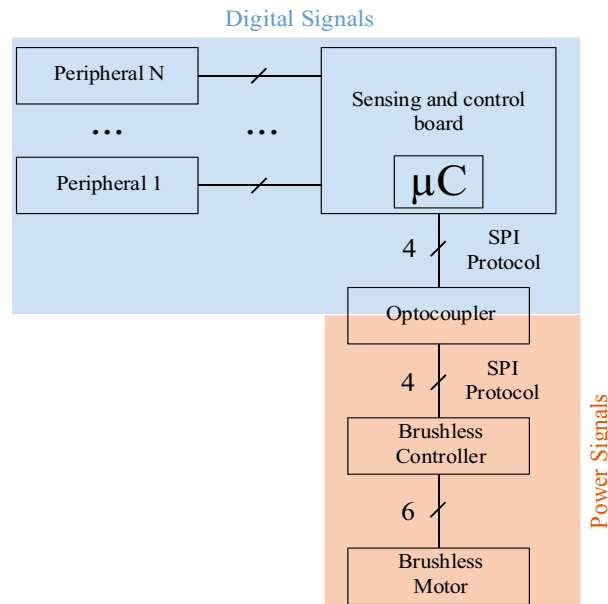


Figure 4.4: Close up of separated grounds between power signals and logical signals

The voltage provided by two batteries of 4 Li-Po cells, are applied to the BLDC motor by means of 6 N-Channel Power MOSFET, whose major role is delivered to the motor phases a PWM voltage. On the other hand, the BLDC controller as well as BLDC integrated Hall sensors must be supplied by a voltage whose ground is the power ground. Thus, since these 2 components have a nominal voltage of 5V, a KF50B 5V linear regulator is used in order to provide the proper voltage.

The logical signals in the control unit are all supplied by means of 7,5V, which are obtained from a step down DC to DC conversion, already implemented in CAMBADA@Home robot platform. Hence, since the logical circuits are supplied at 3.3V while the absolute encoder and optocouplers are supplied at 5V, it is required to use 2 voltage regulators - the first one a 5V linear regulator and the second one a 3.3V linear regulator. Therefore, the KF50B is used either in this approach and the 3.3V linear regulator is a MCP-1703, by Microchip.

4.3.2 Communication Protocols

As aforementioned in Section 4.2, there are some protocols that the control unit must implement to communicate with the sensors and actuators. Herewith, CAN, asynchronous serial communications, SPI and series protocols have to be implemented, using inner peripherals of the μC and external components to fulfill the protocols features.

The CAN protocol is totally implemented by the μC , however there is an external transceiver to interface the μC and the CAN bus, the MAX-3051 circuit.

Both TTL Level and RS-485 communications are assured by internal μC UARTs with the assistance of the MC74LCX125 buffer and the MAX-3362 transceiver, respectively.

On the other hand, the communication between the PIC32MX795F512H and the BLDC controller is made by means of a SPI protocol, which is leaded by a μC inner peripheral.

Furthermore, the serial bit stream generated for read the absolute encoder information is implemented using three μC pins without the assistance of any inner peripheral and/or external transceiver.

The communication necessary to program the μC is assured by unique pins, which are directly connected to a programming tool, while the debugging system uses a UART inner peripheral to communicate over an USB BUS, after usb-serial conversion, obviously. Figure 4.5 helps at clarifying the facts mentioned above.

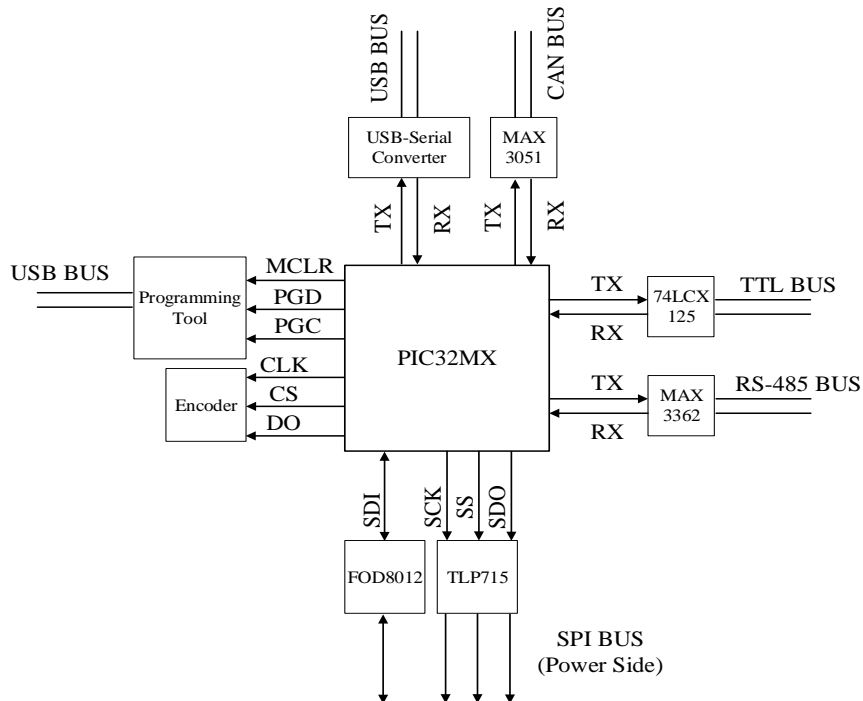


Figure 4.5: Communication architecture overview

4.3.3 Sensing and Control Board

The sections above describe the hardware implementation used for interfacing the μC with the actuators and sensors present in this project. Without despise transceivers and drivers, such as MAX3051, MAX3368 and even MC74LCX125 device, the PIC32MX795F512H is the main controller, which lead all the processes around the manipulator low-level. A central component in this platform is the oscillator, a 8MHz crystal which provide a reference frequency for posterior frequency clock of the μC . The sensing and control board developed contains a large diversity of components, each one with its own mission and chosen by a conjugation of factors, such as price, functionality, size, available stock and author's preference.

The components size is an important project issue, since to have an acceptable control board size, it is fundamental to have components small enough to not over dimension the final product as well as large enough to be welded by hand. In this sense, the majority of the components are Surface-mount Devices (SMD's), which allow the utilization of the two sides of a two-layers Print Circuit Board (PCB), creating an higher density of components per volume.

The electronic components perform a major role in this control unit, however one must take into account the connectors used to link that to the others robot components as well as to the sensors and actuators. It is important that these connectors have some robustness in order to maintain their position with all motions of the robot, avoiding accidental disconnections. Another issue that matters in this topic is the current acceptance by the connector, since their contacts must have enough surface to handle the current through them. Herewith, the connectors for logic signals used in this project have a lock pin and the connectors for power signals are large enough to hold an high current, which can achieve, for instance, up to 70 A in the motor start.

Long last, figure 4.6 depicts all peripheral connections using the μC pins, as well as the indication of the peripherals involved.

4.4 Software Implementation

All software produced in this project is developed using the MPLABX IDE, by Microchip. To compile all C files is used the XC32 compiler, version 1.22.

4.4.1 Microprocessor Initialization

The Microprocessor is the process unit of the platform developed, thus an initialization algorithm must be implemented in order to prepared the μC I/O as well as initialize all needed peripherals. The μC initialization follows these steps:

- Configure analog ports as digital ports, since this project does not use the first ones
- Configure digital ports as inputs or outputs, as peripheral needs
- Configure three UART modules, one SPI module and one CAN module to a desired operation model

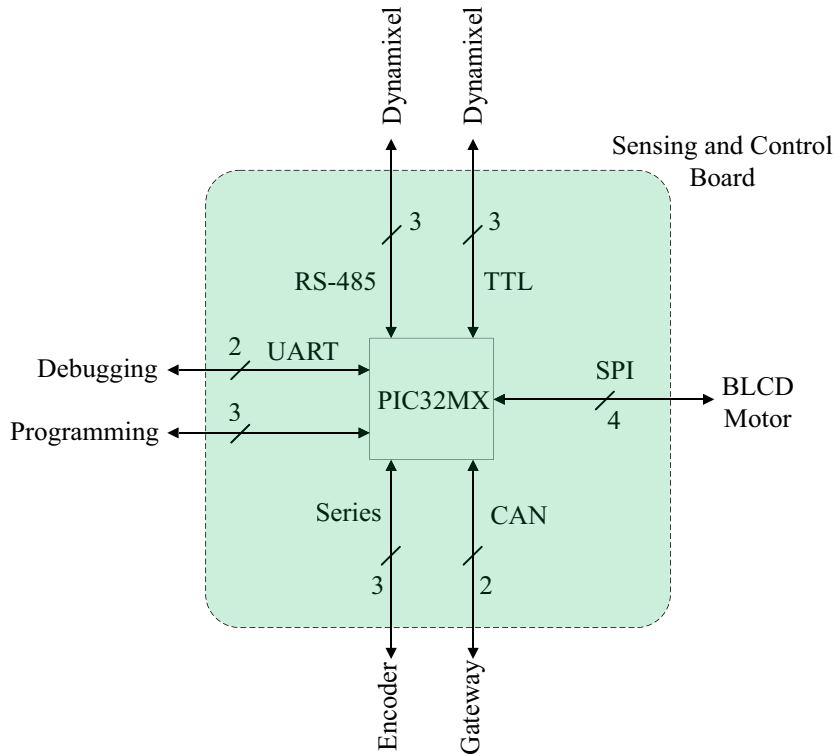


Figure 4.6: Close up of μC connections in sensing and control board

4.4.2 FCM8201 Initialization

The FCM8201 BLDC motor controller needs a toggle sequence to enter in SPI mode, i.e., on power up reset this controller is in stand alone mode and it is necessary change it to SPI mode. Thus, pin 7 and 8 of FCM8201 are used to that purpose, thus the μC leads the generation of a sequence determined by the controller manufacturer.

Furthermore, it is required to program several registers of the FCM8201, in order to choose several rotation and control options, present in the controller operations mode.

4.4.3 Dynamixel Chain Initialization

The Dynamixel servo motors have a powerful inner control which allow the user to configure several movement parameters such as the range of the movement, the maximum torque acceptable, the Proportional Integral Derivative (PID) controller parameters and even the mode of movement, i.e., if the servo is applied for wheel mode or joint mode. Therefore, several initializations must be made to prevent the manipulator to execute movements that could damage its mechanical structure. On the other hand, since the shoulder pitch joint is composed of two MX-106 Dynamixel, it is imperative that one of them operates as a slave and the other one as a master. Besides, these two actuators must be configured to actuate in reverse mode, i.e., the PWM applied at one is the same applied at another, however in opposite direction.

Figure 4.7 shows the main functions of the developed software.

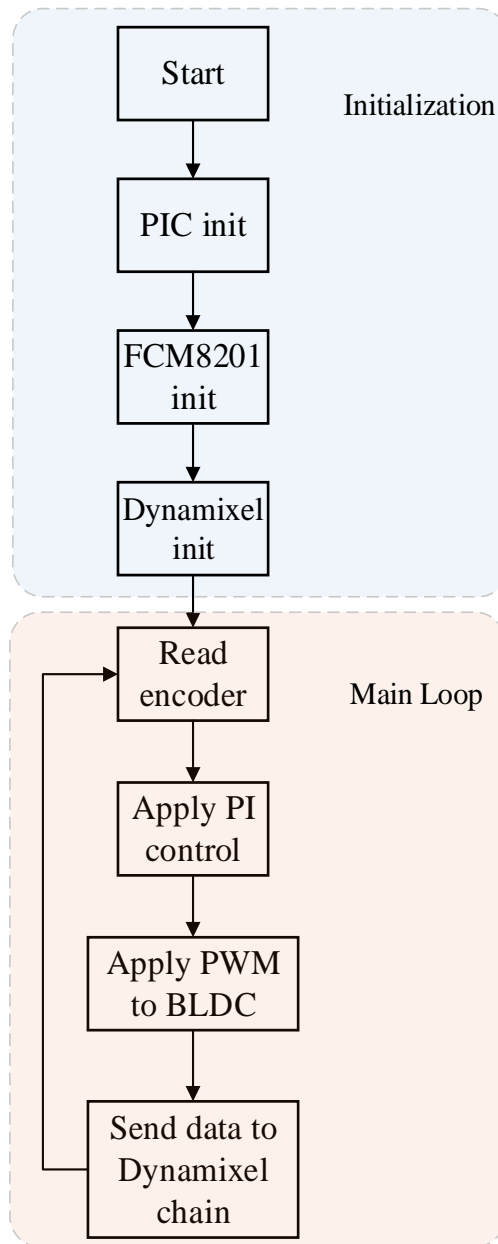


Figure 4.7: Flowchart of the developed software main functions

4.5 Summary

This chapter presents the entire architecture and design, in terms of hardware and software, that was developed in order to control the anthropomorphic manipulator, i.e., control in an efficient manner all rotative joints that compose the anthropomorphic arm.

Since the design present in this dissertation falls on two main types of actuators, a BLDC

motor and several Dynamixel servo motors, different low level controllers was implemented to handling both of them. Moreover, proper interfaces were developed to handle the encoder data out bit stream as well as communicate with the BLDC controller, FCM8201.

Chapter 5

Experimental Results

In this chapter it is presented some results of tests executed during the implementation of the project depict in this document. Therefore, graphics, oscilloscope signals images and other figures are shown to a better comprehension and demonstration.

5.1 Dynamixel actuation

Dynamixel servo motors allow a wide range of communication baud rates, from 9600 bps until 1Mbps. In this sense, send orders and obtain servos feedback can take more or less time, according the user needs. Besides this fact, Dynamixel actuators have a configurable return status delay, which consists on the amount of time between the reception of the message and the response to it, by the servo motor. This time can vary from many μs to ca. 600 μs . Figure 5.1 shows messages being transmitted at 57600 bps and at 250000 bps as well as a variation of the return status delay. The communication baud rates should not exceed 350000 bps, since the bus capacitance could lead to erroneous messages.

Furthermore, Dynamixel actuators have three distinct manners of being actuated, i.e., different approaches aiming at writing a goal position and a goal speed on Dynamixel inner registers, in order to generate a movement:

- Write of goal position and speed in proper Dynamixel registers, one servo at a time. The servo performs the movement after send a status message;
- Write of goal position and speed in several servos and send an action command that enables a simultaneous movement (Write plus Action approach)
- Write goal position and speed simultaneously in several servos by transmitting one only broadcast message (Synchronous Write approach)

The main difference between the first approach and the second one is the fact that writing position and speed data at a Dynamixel once a time results in a delay of actuation between servo motors. This fact could be not desired in many applications, such as Dynamixel chains. The second approach presents a solution to that fact, since it enables the motor torque of desired Dynamixel only when an action message is sending. Furthermore, the first manner described for actuating Dynamixel servo is quite efficient when a chain with many servo motors is used, since with just a one message one can send position and speed data to a group of servo motors.

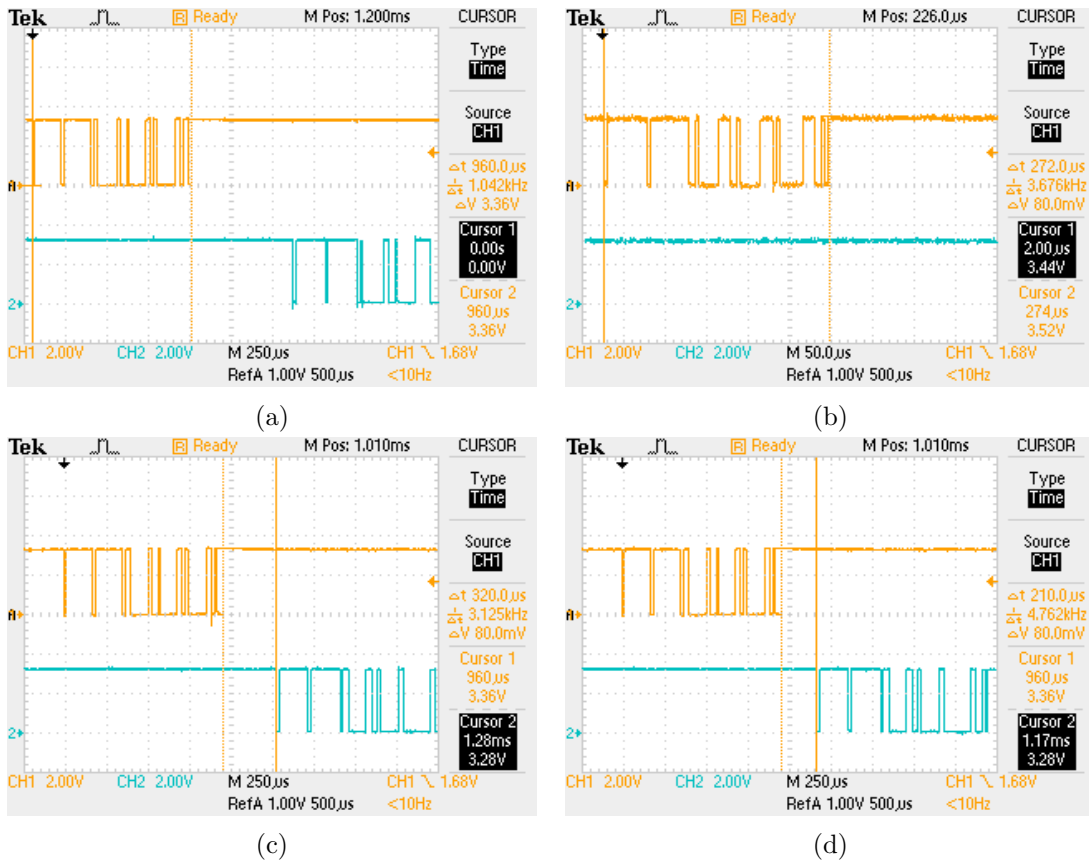


Figure 5.1: a) Transmitted message at 57600 bps b) Transmitted message at 250000 bps c) Transmitted message at 57600 bps with return status delay of 320 μ s d) Transmitted message at 57600 bps with return status delay of 210 μ s

Evaluating figure 5.2 one can determine the total time of transmitting a message just to one servo motor, at baud rate of 57600 bps.

The total actuation time includes sending the message, the status return delay and the time of the return message. At this baud rate the total time is 2.64 ms. Note that, for actuating N servos, it is necessary N times 2.64 ms from the start of the message until the actuation of the last servo motor.

Considering the second approach aforementioned of actuating Dynamixel servos, it is possible write the position and speed data to all desired servo motors, and then send an action command that enables the movement in all motors. Thus, one can assure a simultaneous actuation. Figure 5.3 shows an implementation of this approach, both for a chain of two servo motors and three servo motors.

Assessing last figure one can determine that with the Write plus Action approach one can actuate in two Dynamixel servos within 8.4 ms and in three Dynamixel servos within 12.6 ms. Comparing with the first approach, which presents a lag of actuation of 5.28 ms and 7.92 ms for two and three servos, respectively, this second implementation is ca. 63 % slower, i.e., takes more 63 % of the time to actuate in the same number of servos. However, in an application that requires simultaneous actuation, it is crucial implement this second approach.

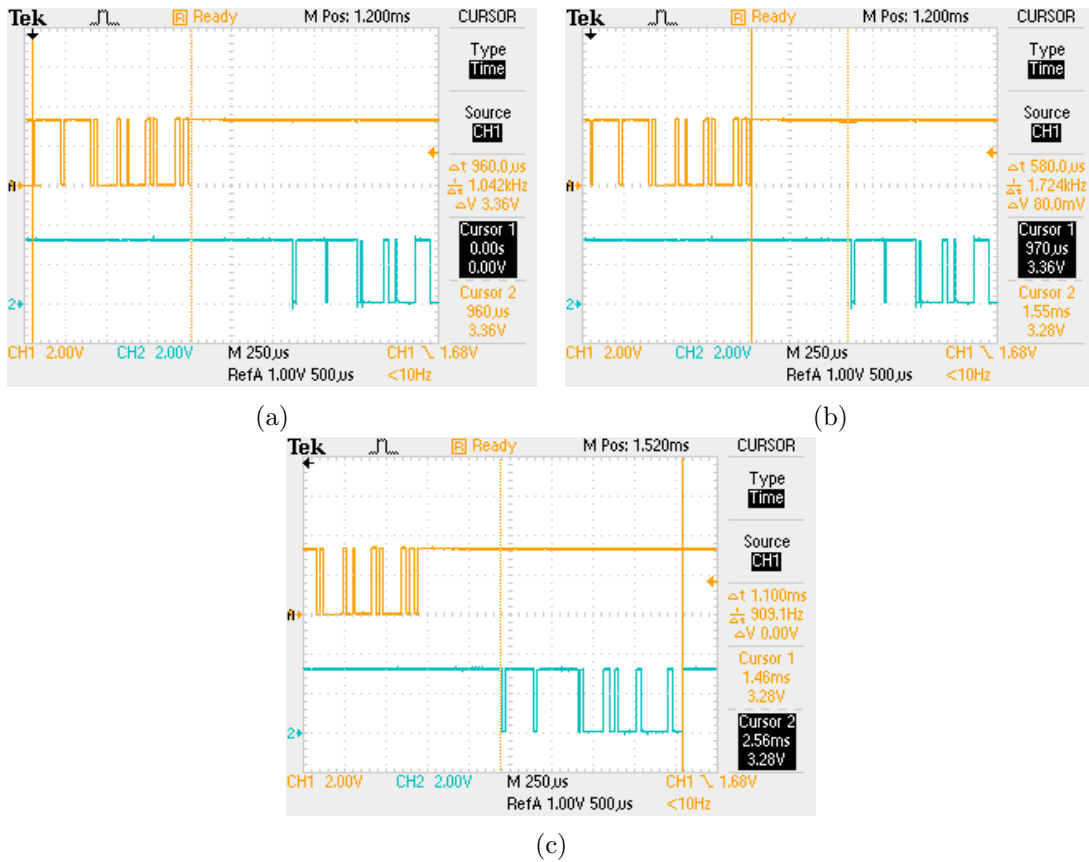


Figure 5.2: a) Transmitted message at 57600 bps (duration of 960 μs) b) Return time delay of 580 μs c) Response message at 57600 bps (duration of 1.1 ms)

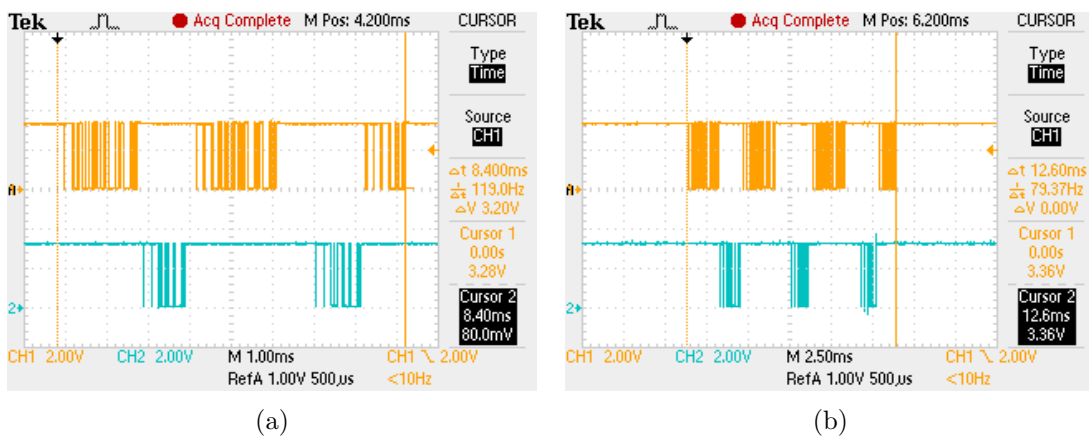


Figure 5.3: a) Write plus Action actuation approach with 2 servo motors b) Write plus Action actuation approach with 3 servo motors

Finally, the third implementation is design for a group of Dynamixel. It consists in a message that contains desired position and speed of several Dynamixel. Thus, the actuation jitter is reduced, allowing better performance in servo motors chains, like the implementation

described in this document. Figure 5.4 depict the messages produced implementing this third methodology. Note that there is no response from the servo motor, since the message produced is sent in broadcast.

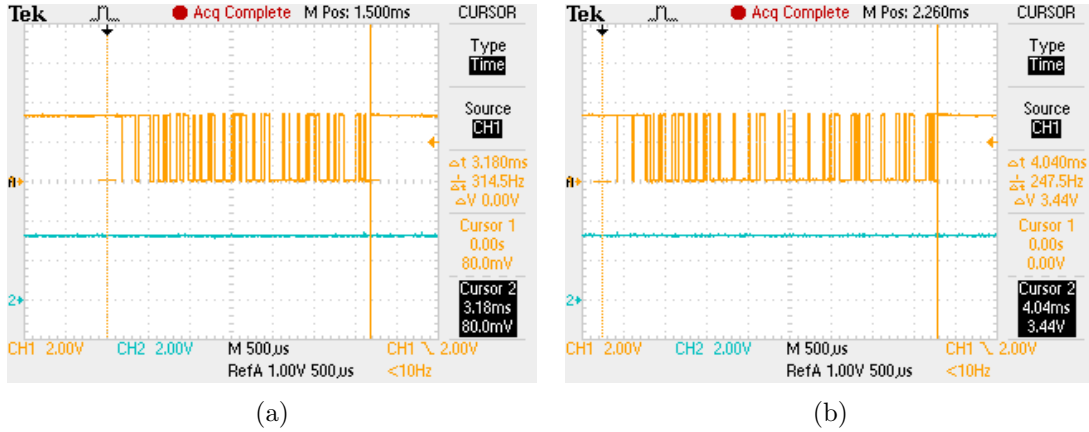


Figure 5.4: a) Synchronous actuation approach with 2 servo motors b) Synchronous actuation approach with 3 servo motors

Assessing the last figure, one can see that actuation lag for two servo motors is 3.18 ms and for three servo motors is 4.04 ms. Relatively to the first approach it represents approximately 60% of time saving.

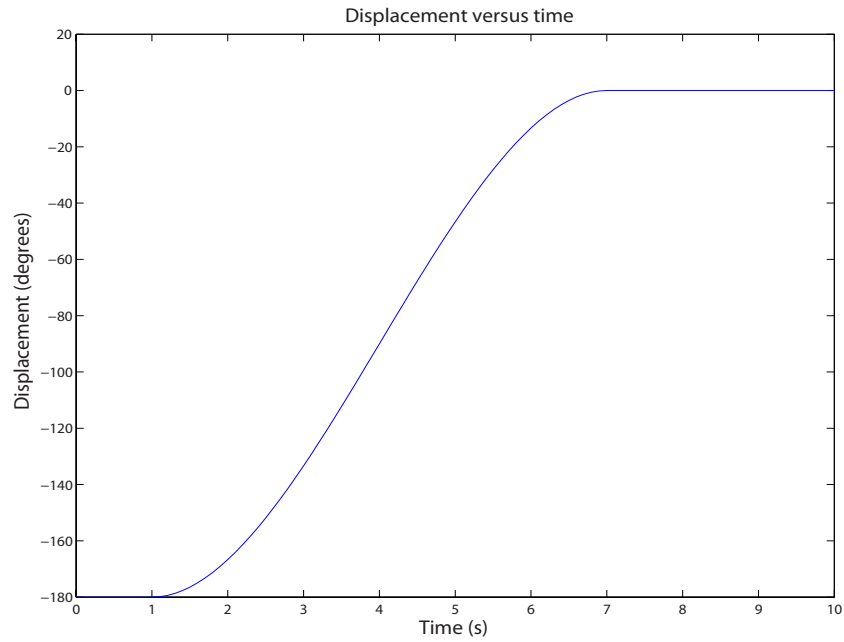
5.2 BLDC step response

It is crucial that the manipulator structure depicted in this document have a low level control, which is able to take the anthropomorphic arm to a desired position. It is possible to have a control loop, receiving position data from the absolute encoder and control the BLDC speed by acting at its FCM8201 controller. Herewith, the author adopted an Proportional Integral (PI) controller, which can complete the chore at acceptable levels. Note that, initially, the control design idea was an PID controller, however during the controller tuning the author realized that the derivative component did not perform a crucial role.

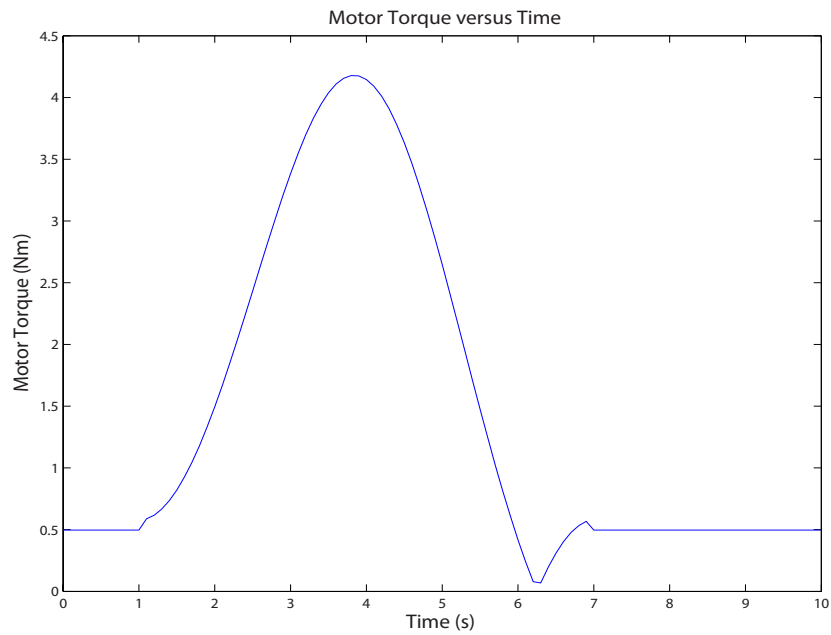
To evaluate some step responses it is fundamental that the BLDC motor have a load, which must cause the same impact as the anthropomorphic structure. In this sense, since the CAD tool used for design the mechanical structure of the anthropomorphic arm owns a integrated simulator, it is quite useful to assess the magnitude of the torque that the BLDC motor must produce to move the manipulator. Figure 5.5a and figure 5.5b show the results of a simulation: displacement in degrees and the respective torque produced by the BLDC aiming at completing the movement, respectively.

As one can see the motor torque achieves 4 Nm when the anthropomorphic arm passes for the 90 degrees angle, i.e., when it is all outstretched and parallel to the ground. Since the setup used for tests is depicted in figure 5.5, the weight of the mass that produces equivalent results could be calculated using equation 5.1.

$$T = F \cdot r \Leftrightarrow T = Mgr \quad [Nm] \quad (5.1)$$



(a) Displacement over time



(b) Torque produced by the BLDC Motor

In this case r takes the value of $32\text{mm} = 0.032\text{m}$ and obviously the d_1 indicated in figure 5.5 is $64\text{mm} = 0.064\text{m}$.

A mass with approximately 12.75 Kg in the setup assembled can simulate the anthropomorphic arm, in the point of view of BLDC torque needed. Thus, the author did several tests with a mass of 13 Kg, namely displacements of 45, 90 and 180 degrees, both clockwise and counterclockwise directions, i.e., with the force produced by the mass acting on

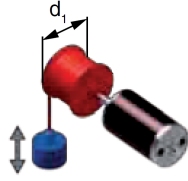


Figure 5.5: Setup assembled for tests, adapted from [43]

behalf of the movement and the force produced by the mass acting opposite to the movement. The results for the three displacements are represented in figures 5.6, 5.7 and 5.8 .

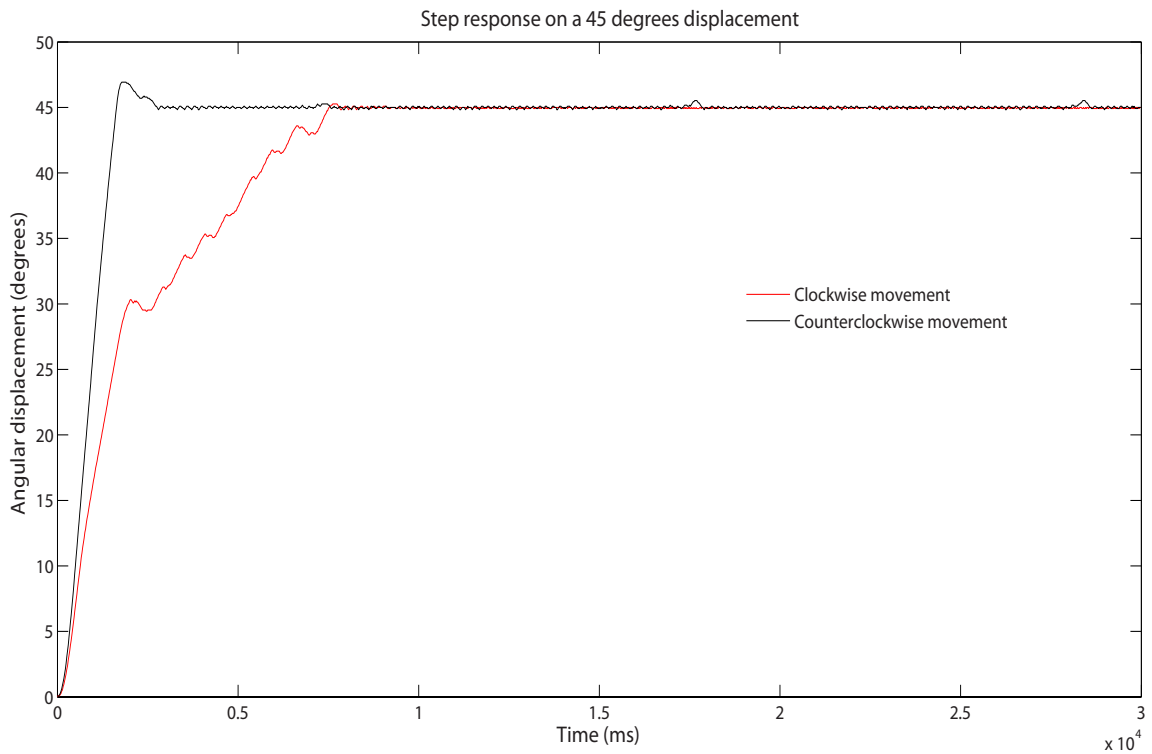


Figure 5.6: Step responses for 45 degrees displacement

5.3 Summary

This chapter presents some experimental results obtained for better modeling the anthropomorphic arm behavior. Although the mechanical structure is not implemented physically, a CAD model allows predict some major variables of the system. Since this project contemplates two types of actuators, BLDC motor and Dynamixel servo motor, these two types behavior were studied in this chapter.

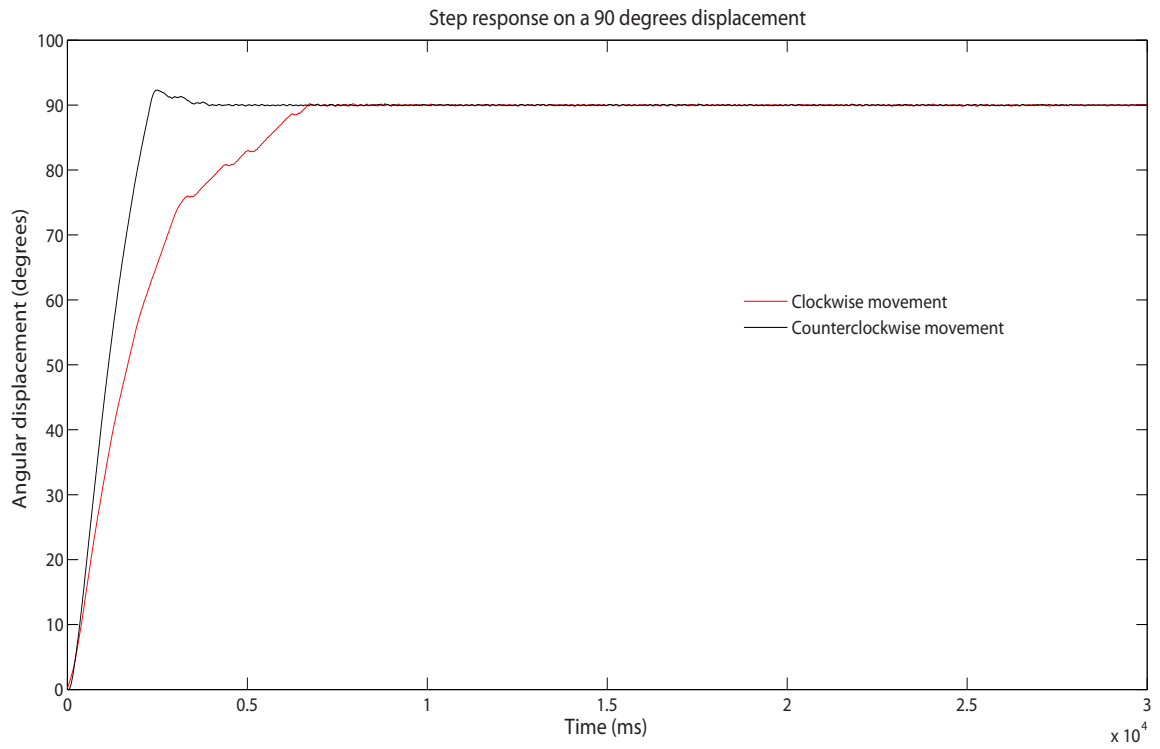


Figure 5.7: Step response for 90 degrees displacement

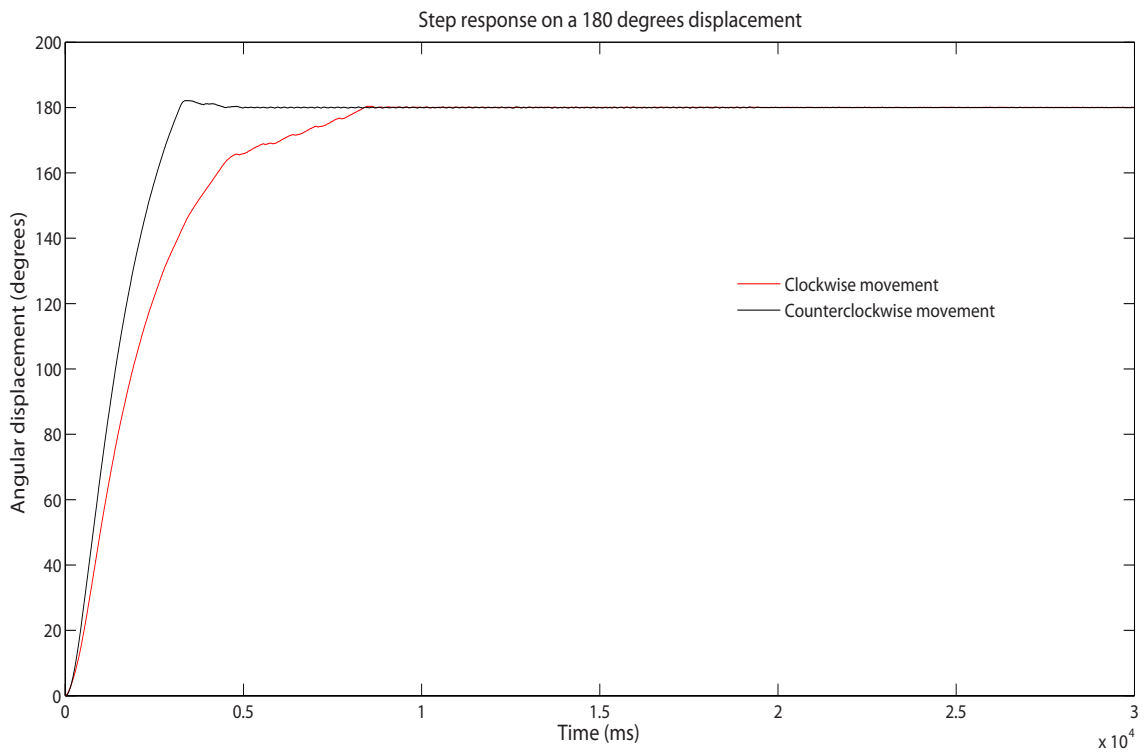


Figure 5.8: Step response for 180 degrees displacement

Chapter 6

Conclusion and Future Work

6.1 Conclusion

The BLDC controller, FCM8201, proved to be a good solution for control BLDC motors with Hall sensors, fulfilling the requirements imposed for the motor manufacturer. On the other hand, the absolute encoder with 12 bits performs an excellent role in this project, since it enable the control position with good precision.

Dynamixel servo motors have a very versatile interface, thus allowing a numerous configurations of control variables as well as assessing important values during the motor operation, which allow a better controlling of all the movement process. The communication protocol is well known and documented, which enable a better knowing of all requirements to perform a good and secure communication.

The μC used, the PIC32MX795F512H, has several and varied inner peripherals, ideal for a develop a project from scratch. Furthermore, this device has a powerful processor as well as a large memory, both RAM and Flash. These features combined with good tools and documentations are a major asset for every project.

Finally, the CAD software used has a set of very important tools that allow a precision analysis of mechanical structure behavior. By configuring material density or even assign a weight in each part, one can simulate various movements and assess numerous variables, in order to a precision prediction of the real world behavior. Thus, these simulations represent a major asset to the project, since one can correct erroneous assemblies thus avoiding waste of material.

6.2 Future Work

There are plenty of ways to improve this project, giving it new and better features.

First of all, in the near future, all mechanical parts designed must be manufactured and assembled, in order to provide the robot with the final mechanical structure of the anthropomorphic arm.

On the other hand, the grabber must be added to the arm mechanical structure model in order to complete the anthropomorphic arm structure. With the grabber model, one can perform new tests to assess the arm behavior as well as create another software layer that is capable of make some simple movements.

Finally, the communication between the low level of electronics developed and the main processor unit of the robot must be defined, i.e., define the messages structure that the main processor sends to the low level electronics and define in low level electronics how to parse these messages in order to complete the desired commands.

Bibliography

- [1] The RoboCup Federation. A Brief History of RoboCup. <http://www.robocup.org/about-robocup/a-brief-history-of-robocup/#>.
- [2] João Cunha, António J. R. Neves, José Luís Azevedo, Bernardo Cunha, Nuno Lau, Artur Pereira, and António Teixeira. A mobile robotic platform for elderly care. *AAL workshop, BIOSTEC 2011*, 2011.
- [3] João Alexandre da Silva Costa e Cunha. Holonomic control and behaviours for the CAMBADA robotic soccer team. Master's thesis, DETI/UA, University of Aveiro, 2009.
- [4] RoboCup2013. Participants robocup@home league. <http://www.robocup2013.org/participants-robocuphome/>, 2013.
- [5] RoboCup2013. RoboCup@home finals with Tech United's AMIGO at the World Championship finals of RoboCup 2013 in Eindhoven (NL). <http://www.flickr.com/photos/robocup2013/9174612362/in/set-72157634359631231>, 2013.
- [6] J. Cunha, J. L. Azevedo, M. B. Cunha, P. Fonseca, N. Lau, C. Martins, C. Moura, A. J. R. Neves, E. Pedrosa, A. Pereira, and A. J. S. Teixeira. CAMBADA@Home'2012: Team Description Paper. 2012.
- [7] J. Cunha, J. L. Azevedo, M. B. Cunha, L. Ferreira, P. Fonseca, N. Lau, C. Martins, A. J. R. Neves, E. Pedrosa, A. Pereira, L. Santos, and A. J. S. Teixeira. CAMBADA@Home'2013: Team Description Paper. 2013.
- [8] Carnegie Mellon University's School of Computer Science. Unimate. <http://www.robotalloffame.org/inductees/03inductees/unimate.html>, 2003.
- [9] Occupational Safety & Health Administration. OSHA Technical Manual (OTM). https://www.osha.gov/dts/osta/otm/otm_iv/otm_iv_4.html, 1999.
- [10] Practical Robotic Services LLC. the start of a revolution... <http://www.ar2.com/>.
- [11] Shimon Y. Nof. *Handbook of Industrial Robotics*, chapter 2nd, pages 54–59. John Wiley & Sons, Inc, 2nd edition, 1999.
- [12] Shimon Y. Nof. *Handbook of Industrial Robotics*, chapter 64th, pages 1201–1212. John Wiley & Sons, Inc, 2nd edition, 1999.
- [13] IEEE Canada. The Shuttle Remote Manipulator System - The Canadarm. http://www.ieee.ca/millennium/canadarm/canadarm_technical.html.

- [14] European Space Agency. European Robotic Arm. http://www.esa.int/Our_Activities/Human_Spaceflight/International_Space_Station/European_Robotic_Arm, 2013.
- [15] Eindhoven University of Technology. AMIGO. <http://www.roboticopenplatform.org/wiki/AMIGO>, February 2013. Robotic Open Platform (ROP).
- [16] J. J. M. Lunenburg, S. A. M. Coenen, S. van den Dries, J. Elfring, R. J. M. Janssen, J. H. Sandee, and M. J. G. van de Molengraft. Tech United Eindhoven Team Description 2013. 2013.
- [17] Eindhoven University of Technology. AMIGO Arms. http://www.roboticopenplatform.org/wiki/AMIGO_Arms, February 2013. Robotic Open Platform (ROP).
- [18] Viktor Seib, Florian Kathe, Daniel Mc Stay, Stephan Manthe, Arne Peters, Benedikt Jöbgen, Raphael Memmesheimer, Tatjana Jakowlewa, Caroline Vieweg, Sebastian Stümper, Sebastian Günter, Simor Müller, Alruna Veith, Michael Kusenbach, Malte Knauf, and Dietrich Paulus. RoboCup 2013 - homer@UniKoblenz (Germany). 2013.
- [19] Leon Ziegler, Jens Wittrowski, Matthias Schöpfer, Frederic Siepmann, and Sven Wachsmuth. ToBI - Team of Bielefeld: The Human-Robot Interaction System for RoboCup@Home 2013. 2013.
- [20] Neuronics AG. Company and Product. http://www.aai.ca/robots/h_arm_ppt_eng.pdf. pages 3-6.
- [21] Xiaoping Chen, Feng Wang, Hao Sun, Jiongkun Xie, Min Cheng, and Kai Chen. KeJia: The Integrated Intelligent Robot for RoboCup@Home 2013. 2013.
- [22] Luís A. Pineda, Iván V. Meza, Gibrán Fuentes, Caleb Rascón, Maria Peña, Hernando Ortega, Mauricio Reyes Castillo, Lisset Salinas, Joel Durán Ortega, Arturo Rodríguez-García, and Varinia Estrada. The Golem Team, RoboCup@Home 2013. 2013.
- [23] HONDA. ASIMO (2011 -) Key Specifications. <http://world.honda.com/ASIMO/technology/2011/specification/>. Accessed in July 2013.
- [24] Fraunhofer IPA. Care-O-bot research, Technical data. <http://www.care-o-bot-research.org/care-o-bot-3/technical-data>. Accessed in July 2013.
- [25] Fraunhofer IPA. Care-O-bot® 3 Download, Products Sheet and Media Information. http://www.care-o-bot.de/Bilder/Care_0_bot_3-frei.jpg. Accessed in July 2013.
- [26] Wim Meeussen, Melonee Wise, Stuart Glaser, Sachin Chitta, Conor McGann, Patrick Mihelich, Eitan Marder-Eppstein, Marius Muja, Victor Eruhimov, Tully Foote, John Hsu, Radu Bogdan Rusu, Bhaskara Marthi, Gary Bradski, Kurt Konolige, Brian Gerkey, and Eric Berger. Autonomous Door Opening and Plugging In with a Personal Robot. *IEEE International Conference on Robotics and Automation*, May 2010.
- [27] Willow Garage. PR2 - Hardware Specs. <http://www.willowgarage.com/pages/pr2/specs>. Accessed in July 2013.

- [28] Jörg Stückler, David Droschel, Kathrin Gräve, Dirk Holz, Michael Schreiber, and Sven Behnke. NimbRo@Home 2013 Team Description. 2013.
- [29] Jörg Stückler, Kathrin Gräve, Jochen Kläβ, Sebastian Muszynski, Michael Schreiber, Oliver Tischler, Ralf Waldukat, and Sven Behnke. Dynamaid: Towards a Personal Robot that Helps with Household Chores. *Proceedings of the 2012 IEEE International Workshop on Advanced Robotics and its Social Impacts*, May 2012.
- [30] Jörg Stückler, David Dröschel, Kathrin Gräve, Dirk Holz, Michael Schreiber, and Sven Behnke. NimbRo@Home 2011 Team Description. 2011.
- [31] Jörg Stückler, Ricarda Steffens, Dirk Holz, and Sven Behnke. Efficient 3D Object Perception and Grasp Planning for Mobile Manipulation in Domestic Environments. *Robotics and Autonomous Systems*, October 2012.
- [32] Universität Bonn. Autonomous Intelligent Systems - NimbRo@Home. <http://www.ais.uni-bonn.de/nimbro/@Home/>. Accessed in July 2013.
- [33] J. L. Azevedo, C. Cruz, J. Cunha, M. B. Cunha, N. Lau, C. Martins, A. J. R. Neves, E. Pedrosa, A. Pereira, A. J. S. Teixeira, and M. Antunes. CAMBADA@Home 2011: Team Description Paper. 2011.
- [34] Maxon Motors. **EC 90 flat** \varnothing 90 mm, brushless, 90 Watt, May 2012. Subject to change.
- [35] Festo AG & Co. KG. *Adaptive gripper DHDG*, January 2011. Subject to change.
- [36] Microchip Technology Inc. 32-bit PIC Microcontrollers Products. <http://www.microchip.com/ParamChartSearch/chart.aspx?branchID=211&mid=10&lang=en&pageId=74>. Accessed in September 2013.
- [37] Robotis Dynamixel. **MX-106T / MX-106R**. <http://support.robotis.com/en/>. Accessed in September 2013, v1.14.
- [38] Robotis Dynamixel. **RX-64**. <http://support.robotis.com/en/>. Accessed in September 2013, v1.14.
- [39] Robotis Dynamixel. **RX-28**. <http://support.robotis.com/en/>. Accessed in September 2013, v1.14.
- [40] Avago Technologies. **AEAT-6010/6012 Magnetic Encoder - 10 or 12 bit Angular Detection Device**, August 2011. Data subject to change.
- [41] Maxon Motor AG. *Maxon EC motor - An introduction to brushless DC motors*, 2012. Accessed in April 2013.
- [42] Maxim Integrated Products Inc. *3.3V, High-Speed, RS-485/RS-422 Transceiver in SOT Package*, March 2007. 3rd revision.
- [43] Jan Braun. *Formulae Handbook*, 2012. Maxon Academy.

Appendices

Appendix A

Control Board Schematics and Layouts

This appendix presents the final control board schematic as well as its PCB layout. Both were produced using Cadence OrCAD, version 16.0. Furthermore, this appendix shows top and bottom sides of the first PCB prototype produced.

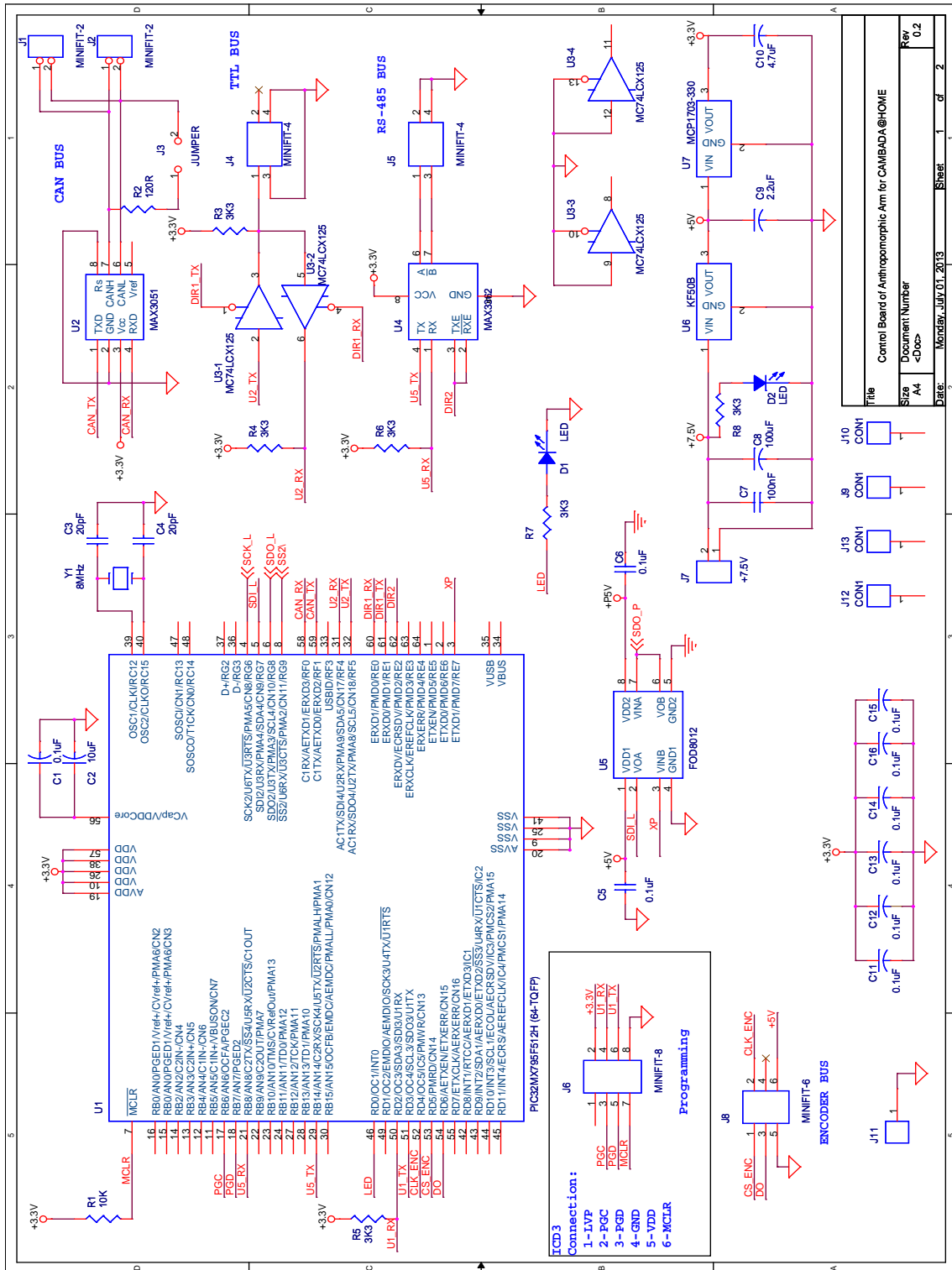


Figure A.1: Final Control Board Schematic - Digital Part

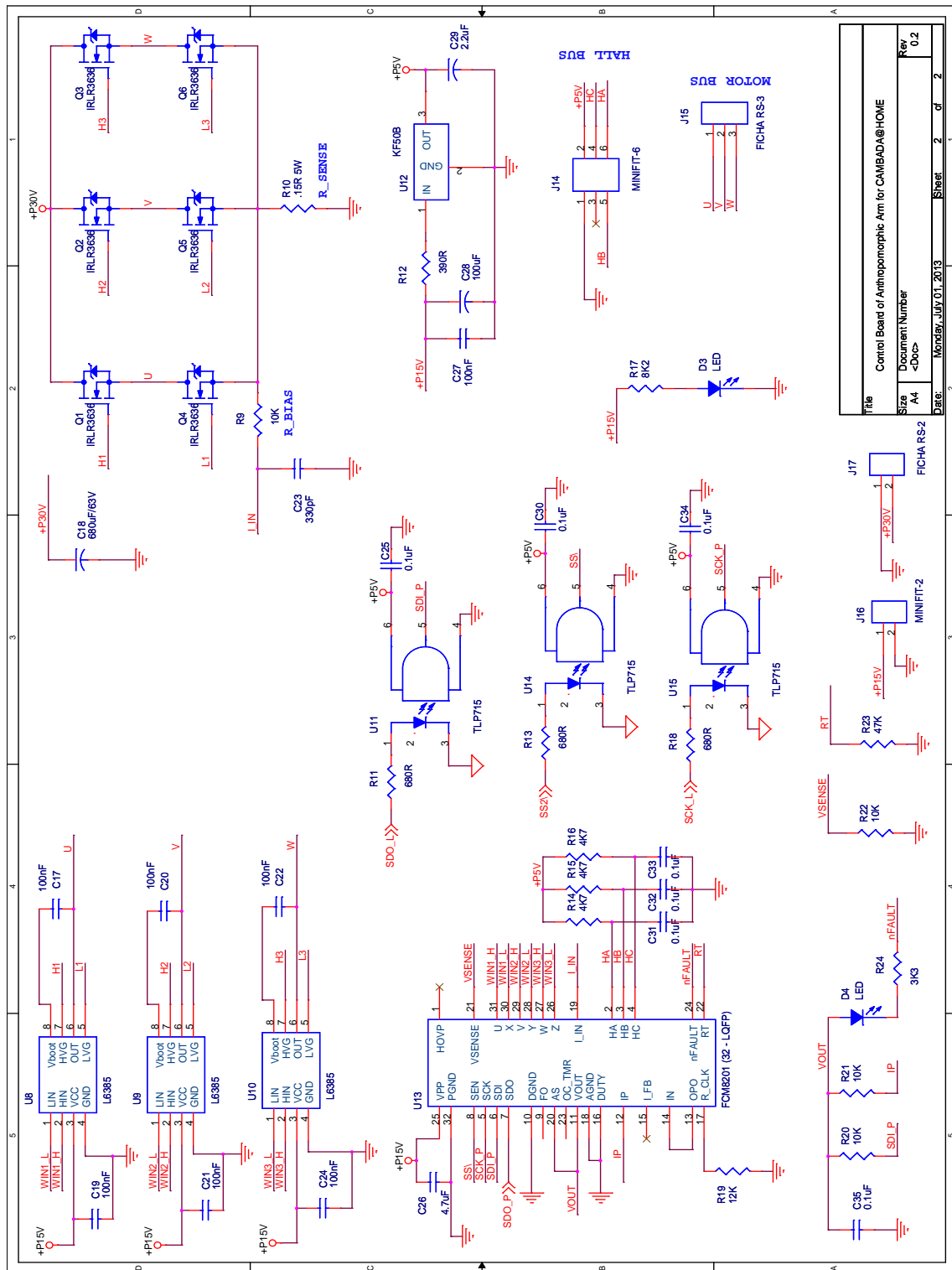


Figure A.2: Final Control Board Schematic - Power Part

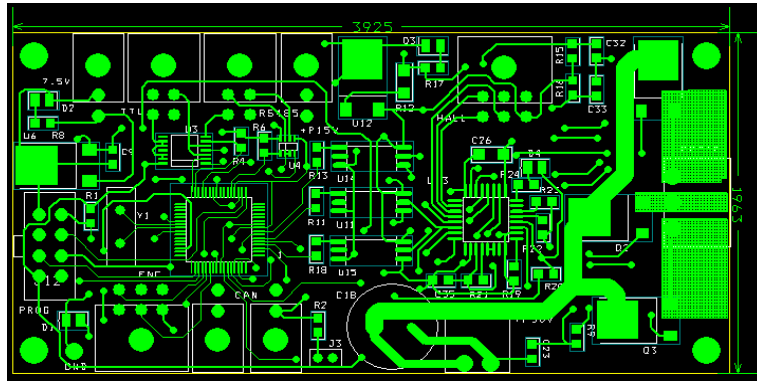


Figure A.3: PCB layout - Top side

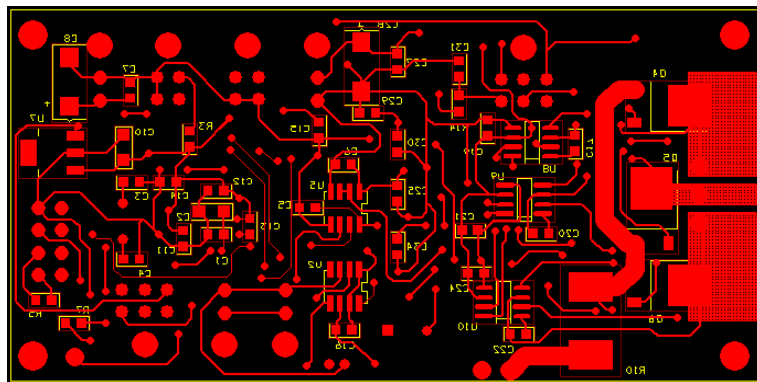


Figure A.4: PCB layout - Bottom side

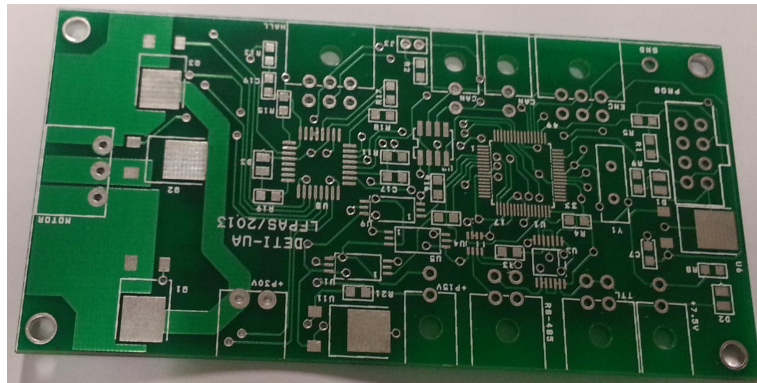


Figure A.5: First PCB prototype - Top Side

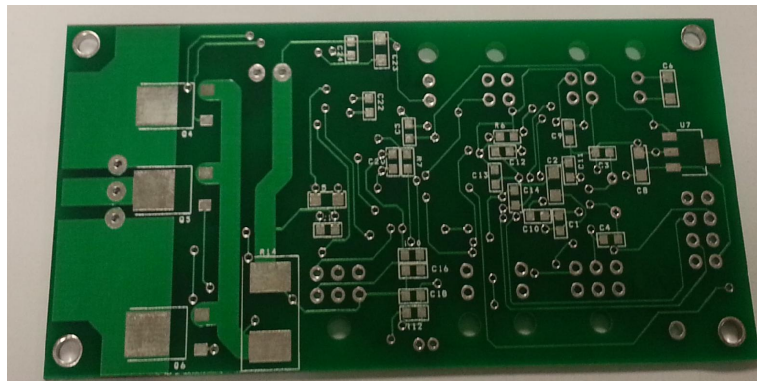


Figure A.6: First PCB prototype - Bottom Side